

UCLA

UCLA Previously Published Works

Title

Abundant ammonia and nitrogen-rich soluble organic matter in samples from asteroid (101955) Bennu

Permalink

<https://escholarship.org/uc/item/51w771pn>

Journal

Nature Astronomy, 9(2)

ISSN

2397-3366

Authors

Glavin, Daniel P

Dworkin, Jason P

Alexander, Conel M O'D

et al.

Publication Date

2025

DOI

10.1038/s41550-024-02472-9

Copyright Information

This work is made available under the terms of a Creative Commons Attribution License, available at <https://creativecommons.org/licenses/by/4.0/>

Peer reviewed

Abundant ammonia and nitrogen-rich soluble organic matter in samples from asteroid (101955) Bennu

Received: 25 July 2024

Accepted: 16 December 2024

Published online: 29 January 2025

 Check for updates

A list of authors and their affiliations appears at the end of the paper

Organic matter in meteorites reveals clues about early Solar System chemistry and the origin of molecules important to life, but terrestrial exposure complicates interpretation. Samples returned from the B-type asteroid Bennu by the Origins, Spectral Interpretation, Resource Identification, and Security–Regolith Explorer mission enabled us to study pristine carbonaceous astromaterial without uncontrolled exposure to Earth’s biosphere. Here we show that Bennu samples are volatile rich, with more carbon, nitrogen and ammonia than samples from asteroid Ryugu and most meteorites. Nitrogen-15 isotopic enrichments indicate that ammonia and other N-containing soluble molecules formed in a cold molecular cloud or the outer protoplanetary disk. We detected amino acids (including 14 of the 20 used in terrestrial biology), amines, formaldehyde, carboxylic acids, polycyclic aromatic hydrocarbons and N-heterocycles (including all five nucleobases found in DNA and RNA), along with ~10,000 N-bearing chemical species. All chiral non-protein amino acids were racemic or nearly so, implying that terrestrial life’s left-handed chirality may not be due to bias in prebiotic molecules delivered by impacts. The relative abundances of amino acids and other soluble organics suggest formation and alteration by low-temperature reactions, possibly in NH_3 -rich fluids. Bennu’s parent asteroid developed in or accreted ices from a reservoir in the outer Solar System where ammonia ice was stable.

Primitive asteroids—those whose bulk chemistry was established in the protoplanetary disk—record processes that occurred during the formation and evolution of the early Solar System. The transport and delivery of organic compounds from these bodies could have been a source of molecules available for the emergence of life on Earth and potentially elsewhere.

Carbonaceous chondrite (CC) meteorites are samples of primitive carbon-rich bodies. In particular, the CI, CM, CR, CY and C₂_{ung} (Ivuna-like, Mighei-like, Renazzo-like, Yamato-like and ungrouped-type-2, respectively) CCs have experienced moderate to extensive aqueous alteration (reactions with liquid water) in their parent bodies and typically contain ~1–3 wt% total carbon, with rare instances up to ~5 wt% (ref. 1). Organic carbon is primarily found in structurally complex insoluble

organic matter and a diverse mixture of soluble organic matter (SOM) that contains prebiotic organic molecules (ref. 2 and the references therein). However, it is often unclear which Solar System objects are the parent bodies of CCs³. Furthermore, they experience alteration upon exposure to the terrestrial environment⁴, making interpretation challenging. The Origins, Spectral Interpretation, Resource Identification, and Security–Regolith Explorer (OSIRIS-REx) mission collected pristine material from the well-characterized surface of primitive B-type asteroid (101955) Bennu and delivered it to Earth under controlled conditions to minimize contamination and protect against atmospheric entry effects⁵.

Spacecraft observations made in proximity to Bennu corroborated preflight predictions^{6,7} of a carbon-rich composition, including strong

✉ e-mail: daniel.p.glavin@nasa.gov

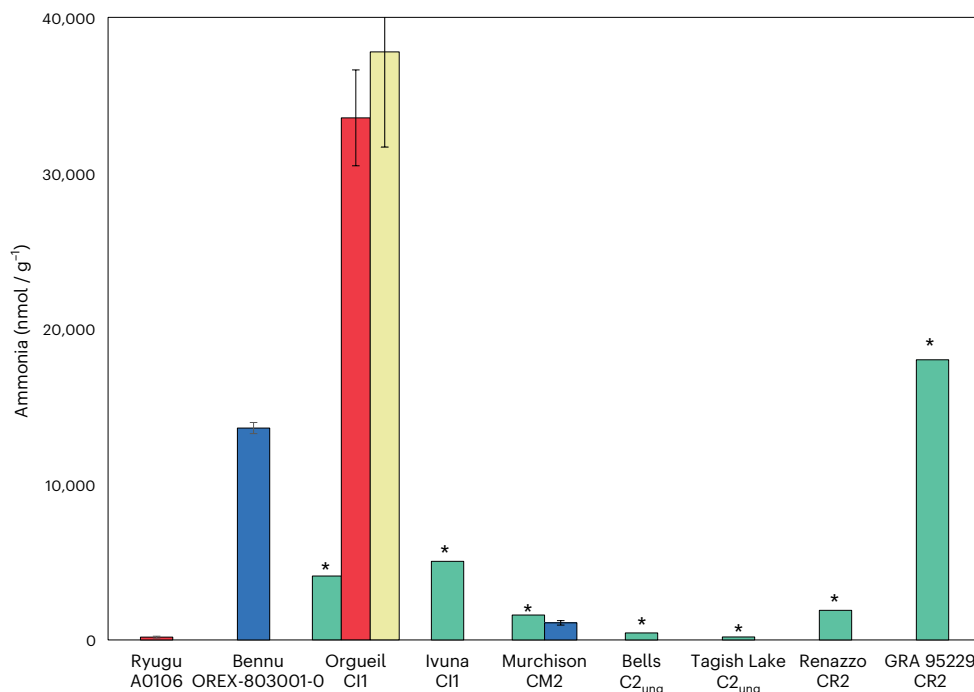


Fig. 1 | Concentrations of free ammonia measured in the extracts of Benu (sample OREX-803001-0), Ryugu (sample A0106) and selected CCs. Data from this study (Extended Data Table 2) for the hot-water extracts of Benu and Murchison (blue bars); data from hot-water extracts of Ryugu and Orgueil²¹ (red bars); data from cold-water leachates of Orgueil²² (yellow bar); and data from water and dichloromethane:methanol (9:1 v/v) extracts of Orgueil, Ivuna, Murchison, Bells, Tagish Lake (lithology not specified), Renazzo and GRA 95229

(ref. 16) (green bars). Data is presented as mean values \pm the standard error of the mean. Estimated concentration of free ammonia is indicated by an asterisk taken from the data shown in Fig. 1a in ref. 16 and did not include errors. The large difference in ammonia concentrations measured in the Orgueil meteorite extracts could be due to differences in the extraction and analytical methods used^{16,21,22} and/or sample heterogeneity.

aliphatic and aromatic organic carbon features at 3.4 μm , consistent with carbon abundances up to ~2.5 wt% and a low-temperature (<100 °C) aqueous alteration history^{8,9}. A much weaker spectral feature observed at 3.1 μm could be consistent with some NH-bearing phases⁹, such as ammonium salts or N-rich organic matter. The remote sensing data also confirmed that Benu is a rubble pile⁷, consisting of reaccumulated fragments of a larger, catastrophically disrupted asteroid (hereafter, parent body).

The spacecraft collected regolith (unconsolidated granular material) from as deep as ~0.5 m in Hokioi crater¹⁰, which is thought to be a recent impact site on Benu based on its redder than average spectral slope¹¹, and it delivered a total sample mass of 121.6 g to Earth⁵. Early laboratory analyses found C contents of 4.5–4.7 wt% and N contents of 0.23–0.25 wt% (ref. 5). The regolith's hydrated mineralogy⁵ suggests that Benu's parent body accreted ices, which condensed from the outer protoplanetary disk.

Given Benu's compositional resemblance to aqueously altered CIs and CMs^{5–9}, we hypothesized¹² that the samples would contain a similar suite of organic compounds—including molecules found in biology, such as protein amino acids with left-handed enantiomeric excesses¹³, carboxylic acids, purines, pyrimidines and their precursors—and similar abundances and distributions of SOM. To test these hypotheses and explore the implications for Benu's parent body, we analysed organic matter in four aggregate (unsorted bulk) Benu samples: two samples consisting of mostly fine particles (<100 μm) retrieved from spillover onto the avionics deck of the sample return canister^{5,12} and two samples containing a mixture of fine and intermediate (100–500 μm) particles removed from inside the Touch-and-Go Sample Acquisition Mechanism (TAGSAM)¹⁴ (Methods).

Results

We conducted elemental analyser–isotope ratio mass spectrometry (EA-IRMS) measurements of Benu aggregates, including a hot-water

extract and solid residue (Methods), and found comparable total abundances of C (4.5–4.7 wt%) and N (0.23–0.25 wt%) as the early analyses⁵ (Extended Data Table 1). The hot-water extract was enriched in ¹⁵N (+180 \pm 47‰) (Extended Data Table 1 and Supplementary Table 4) and had a high concentration of ammonia ~13.6 $\mu\text{mol g}^{-1}$ (Fig. 1 and Extended Data Table 2). The ammonia concentration corresponded to ~40% of the estimated total N in the Benu hot-water extract before dry-down (Extended Data Table 1 and Supplementary Table 4). The large ¹⁵N indicates that the ammonia was not derived from comparatively ¹⁵N-depleted spacecraft hydrazine propellant ($\delta^{15}\text{N} = +4.7\text{‰}$; Supplementary Information).

We performed untargeted analyses of methanol extracts of Benu aggregate using Fourier-transform ion cyclotron resonance–mass spectrometry (FTICR-MS; Methods). The mass spectra of the extracts contained tens of thousands of compounds with mass-to-charge ratios (m/z) between 100 and 700 that correspond to ~16,000 molecular formulae consisting of C, H, N, O, S and Mg (Fig. 2). We identified a continuum of molecular sizes, with a range of carbon oxidation states, from non-polar or slightly polar—including polycyclic aromatic hydrocarbons, alkylated polycyclic aromatic hydrocarbons and a homologous series of unsaturated substituted aliphatic molecules—to more polar small molecules containing only CHO, CHNO, CHOS or CHNOS (Fig. 2, Extended Data Fig. 1 and Supplementary Fig. 15). The SOM is characterized by its nitrogen-rich chemistry, with up to seven nitrogen atoms per molecule detected by means of photoionization (APPI⁺) and electrospray ionization (ESI^{+/+}), respectively (Fig. 2 and Extended Data Fig. 1).

We surveyed for amino acids using pyrolysis gas chromatography–triple quadrupole–mass spectrometry (pyGC-QqQ-MS; Methods and Supplementary Fig. 14). We then determined the abundances and enantiomeric ratios of amino acids in a hot-water extract by means of liquid chromatography with ultraviolet (UV) fluorescence detection

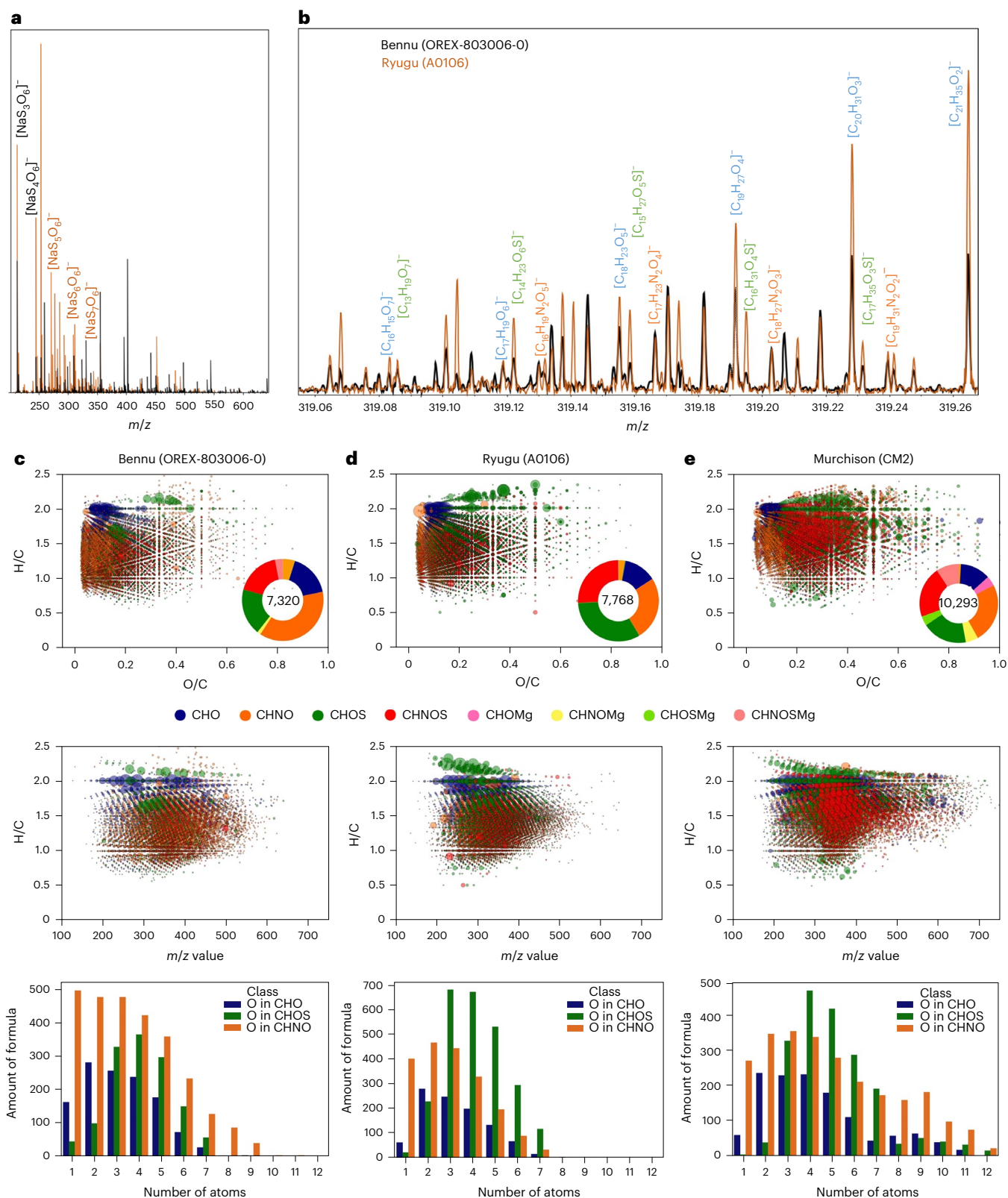


Fig. 2 FTICR-MS data in electrospray ionization mode of the methanol extracts from Benu (OREX-803006-0), compared with Ryugu (A0106) and Murchison. **a**, Mass spectra of Benu (black) and Ryugu (orange) samples showing the relative abundance of polythionates with three to seven S atoms. **b**, Detail around $m/z = 319$ with major annotated elementary compositions (complete annotation can be found in Supplementary Fig. 3). **c–e**, Data visualization of the chemical compositions and number of molecules in Benu (c) compared with Ryugu (d) and Murchison (e). Top, the Van Krevelen diagrams

of H/C versus O/C atomic ratios of the compositional data as obtained from exact mass analysis. Coloured annuli enclose the total number of molecules assigned by mass, with colours indicating the relative abundances of the chemical families. Individual data points use the same colours to specify each family, and the size of each bubble reflects the intensity of the signal from the mass spectrum. Middle, the H/C atomic ratios as a function of m/z from 100 to 700. Bottom, the number of molecular formulae as a function of number of oxygen atoms in the CHO, CHOS and CHNO chemical families.

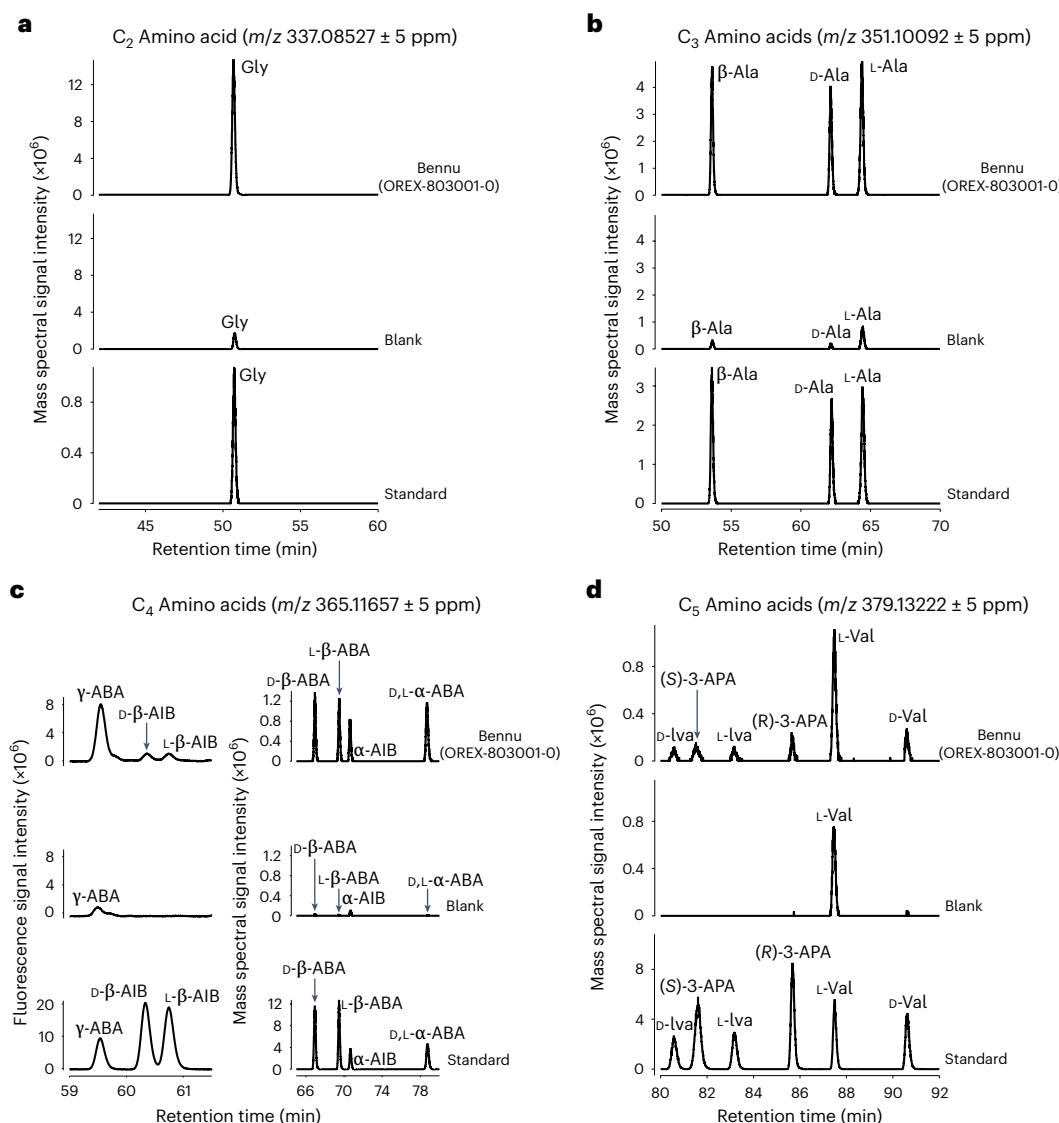


Fig. 3 | Amino acids identified by liquid chromatography mass spectrometry in the acid-hydrolysed, hot-water extract of Bennu (OREX-800031-0).

a–d, Partial chromatograms obtained by LC-FD/HRMS after analysis of the standard and the 6 M HCl-hydrolysed water extracts of the FS-120 (blank) and Bennu (OREX-803001-0). **a**, Single-ion mass chromatograms at m/z 337.08527 corresponding to the C_2 amino acid glycine (Gly). **b**, Single-ion mass chromatograms at m/z 351.10092 corresponding to the C_3 amino acids β -alanine (β -Ala), D-alanine (D-Ala) and L-alanine (L-Ala). **c**, Right, single-ion mass chromatograms at m/z 365.11657 corresponding to the C_4 amino acids D- β -amino- n -butyric acid (D- β -ABA), L- β -amino- n -butyric acid (L- β -ABA), α -aminoisobutyric acid (α -AIB) and D,L- α -amino- n -butyric acid (D,L- α -ABA). Left, the UV

fluorescence separation and detections of the C_4 amino acids γ -amino- n -butyric acid (γ -ABA) and D- and L- β -aminoisobutyric acids (D- and L- β -AIB). These C_4 amino acids were also detected in the single-ion chromatogram at m/z 365.11657; however, a large *o*-phthalaldehyde/N-acetyl-L-cysteine (OPA/NAC) derivative peak eluted at a similar time as these amino acids, suppressing amino acid peak intensities. **d**, Single-ion mass chromatograms at m/z 379.13222 corresponding to the C_5 amino acids D-isovaline (D-Iva), L-isovaline (L-Iva), (S)-3-aminopentanoic acid (S-3-APA), (R)-3-aminopentanoic acid (R-3-APA), L-valine (L-Val) and D-valine (D-Val). The amino acids detected in the blank are likely to be derived from the solvents and derivatization reagents used for sample processing and analysis.

and mass spectrometry (LC-FD/MS; Fig. 3, Methods, Extended Data Fig. 2 and Supplementary Figs. 8 and 9).

A total of 33 amino acids were identified in the Bennu aggregates along with an uncounted suite of C_6 and C_7 aliphatic amino acids that were also detected but were not identified by name with standards (Fig. 3, Extended Data Tables 2 and 3 and Extended Data Fig. 2). These included 14 of the 20 standard protein amino acids used in terrestrial biology (Supplementary Table 12), all previously reported in meteorites¹³. Glycine was the most abundant amino acid (44 nmol g⁻¹), with the majority in a free form, that is, without acid hydrolysis (Extended Data Table 3). Methionine, tyrosine and asparagine were tentatively detected at trace levels above background near the 0.1 nmol g⁻¹ detection limit (Supplementary Table 12).

In addition, 19 non-protein amino acids were identified (Extended Data Table 3 and Supplementary Figs. 6, 8 and 9). All possible isomers of the C_3 to C_5 primary aliphatic amino acids were identified in the hot-water extract, as well as leucine, isoleucine and ϵ -amino- n -caproic acid at trace levels (Fig. 3, Extended Data Table 3 and Supplementary Figs. 8 and 9).

All chiral non-protein amino acids that could be enantiomerically resolved, including isovaline, norvaline, β -amino- n -butyric acid, β -aminoisobutyric acid and 3-aminopentanoic acid, were present as racemic or near racemic mixtures (equal abundances of D- and L-enantiomers) within analytical uncertainties (Extended Data Table 4). The detection of racemic alanine and aspartic acid within error indicates that the sample was pristine, with negligible biological L-protein

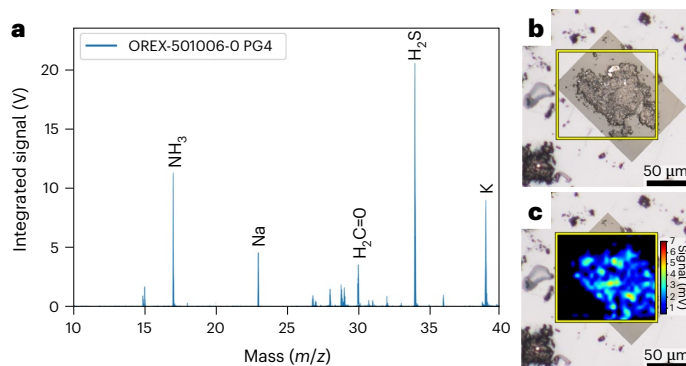


Fig. 4 | Ammonia and formaldehyde in Benu (OREX-501006-0) identified by μ -L²MS. **a**, Summed mass spectrum acquired from several $\sim 100\ \mu\text{m}$ grains mounted on a KBr window with mass peaks for ammonia (NH_3), sodium (Na), formaldehyde ($\text{H}_2\text{C}=\text{O}$), hydrogen sulfide (H_2S) and potassium (K) indicated. Spectrum acquired by μ -L²MS using a vacuum UV photoionization at 118 nm. **b**, Optical mosaic of particle with yellow box demarking region mapped by μ -L²MS. **c**, Spatial map of ammonia distribution overlaid over optical image. The μ -L²MS laser beam spot size was $5\ \mu\text{m}$.

amino acid contamination. An L-valine excess of $\sim 34\%$ was measured in the same hot-water extract after acid hydrolysis (Extended Data Table 4); however, we also observed elevated levels of L-valine in the procedural blank (Fig. 3), so laboratory contamination is a possible explanation. Isotopic measurements of valine will be needed to constrain the origin of the measured L-excess in the Benu extract.

Ammonia and formaldehyde are potential precursors for the synthesis of amino acids and other soluble organic molecules and were key targets for this investigation. Ammonia was independently identified, along with formaldehyde, in an avionics deck sample using micro two-step laser mass spectrometry (μ -L²MS) (Fig. 4 and Methods). Ammonia was also heterogeneously distributed in these particles at the $\sim 5\ \mu\text{m}$ scale (Fig. 4). Most of the ammonia in the Benu aggregate samples was likely to have been originally retained as salts or bound to clay minerals or organic matter^{15,16} because highly volatile free ammonia is prone to loss. Volatile methylamine ($914\ \text{nmol g}^{-1}$) and ethylamine ($121\ \text{nmol g}^{-1}$), which are derivatives of ammonia, dominated the 16 aliphatic primary amines identified in the hot-water extract (Extended Data Table 2 and Supplementary Fig. 6) and were also likely to be present as salts.

Nine C_1 – C_7 monocarboxylic acids and two dicarboxylic acids were identified in the hot-water extract by GC-QqQ-MS (Extended Data Table 5 and Supplementary Fig. 10). Formic ($4,106\ \text{nmol g}^{-1}$) and acetic ($1,436\ \text{nmol g}^{-1}$) acids were the two most abundant carboxylic acids detected.

At least 23 different N-heterocycles, including all five canonical biological nucleobases (adenine, guanine, cytosine, thymine and uracil) (Extended Data Table 6), were identified in an acid extract by high-performance liquid chromatography with electrospray ionization and high-resolution mass spectrometry (HPLC/ESI-HRMS; Methods and Supplementary Figs. 11–13). Many of these N-heterocycles were also detected in aggregate material using wet chemistry pyGC-QqQ-MS (Supplementary Fig. 14).

Discussion

Evidence for extraterrestrial soluble organic matter

The diversity of SOM in the Benu methanol extract (Fig. 2) is inconsistent with terrestrial biology, which has a much simpler distribution¹⁷. The large ^{15}N enrichment ($\delta^{15}\text{N} = +180\text{‰}$; Extended Data Table 1) in the hot-water extract that consisted of ammonia, amines, amino acids, N-heterocycles and other N-containing molecules falls well outside the $\delta^{15}\text{N}$ terrestrial organics range of -10‰ to $+20\text{‰}$ (ref. 18).

The complex distribution of amines, carboxylic acids and mostly racemic amino acids, including several non-protein amino acids that are rare or non-existent in biology (Extended Data Tables 2–5), strongly supports an extraterrestrial origin of these molecules. The violation of Chargaff's rules (1:1 ratio of purine and pyrimidine bases should exist in the DNA of any organism) and diversity of N-heterocycles, including biologically uncommon molecules (Extended Data Table 6), also indicate a non-terrestrial origin.

Benu's volatile-rich nature compared with other astromaterials

The Benu aggregate samples analysed in this study had a higher mass-weighted average abundance of total C and N than previously studied CI and CM meteorites¹⁹ and aggregate samples from Ryugu (Supplementary Table 3). This high volatile content may be related to the formation environment and/or alteration history of Benu's parent body. Although Benu's mineralogy and elemental composition are similar to those of the extensively altered CI1 chondrites⁵, the bulk H and N isotopic compositions (Extended Data Table 1 and Supplementary Fig. 3) suggest a closer affinity to less aqueously altered type-2 chondrites, such as Tagish Lake and Tarda.

The diversity of SOM in the Benu aggregates is comparable with that in Ryugu samples and the CM2 meteorite Murchison^{17,20}, though with a lower mass range and carbon oxidation state than Murchison (Fig. 2 and Extended Data Fig. 1). The nitrogen-rich composition of the Benu aggregates analysed so far contrasts with the sulfur-rich chemistry of the Ryugu samples²⁰, reflecting low-temperature aqueous processing on Benu's parent body and a nitrogen-rich organic chemistry distinct from that of the most aqueously altered CI and CM chondrites.

The water-extracted ammonia abundance that we measured for Benu was 12 times higher than in Murchison and 75 times higher than in Ryugu (Fig. 1 and Extended Data Table 2). It is exceeded only by that of the CR2 Graves Nunataks (GRA) 95229 (ref. 16) and the CI1 Orgueil^{21,22}. A different Orgueil sample extract¹⁶ had much lower free ammonia abundances compared with Benu (Fig. 1). Because hydrothermal treatment at $300\ ^\circ\text{C}$ and $100\ \text{MPa}$ releases additional insoluble organic matter-bound ammonia from these CCs¹⁶, the abundance of ammonia in the Benu hot-water extract is likely to represent a lower limit (Extended Data Table 2). Ammonium salts have also been identified in comet 67P/Churyumov–Gerasimenko^{23,24} and the dwarf planet Ceres²⁵. Carboxylic acids are typically among the most abundant soluble organic compound classes in CCs (Fig. 5)²⁶, and these molecules could have served as the counterions to any ammonium salts in Benu (for example, ammonium formate as observed in comet 67P (refs. 23,24)).

The C_1 – C_6 amine distribution follows the trend of decreasing concentration with increasing size observed in CI1, CM2 and C_2 chondrites (Extended Data Table 2). However, the higher overall abundance and broader distribution of amines compared with Ryugu and Orgueil (Extended Data Table 2) could be explained by a lower degree of aqueous activity during organic synthesis in Benu's parent body. Ryugu samples exhibit a much higher abundance of isopropylamine versus the less thermally stable *n*-propylamine²⁷, whereas the straight-chain and branched amine abundances we measured for Benu were similar to each other (Extended Data Table 2). This observation may also be indicative of less extensive hydrothermal alteration in Benu's parent body.

The Benu hot-water extract displays greater structural diversity of monocarboxylic acids compared with Ryugu with nine C_1 – C_7 carboxylic acids identified (Extended Data Table 5). Although the Ryugu aggregate has much higher total abundances of formic and acetic acids compared with Benu, no other monocarboxylic acids were reported in the Ryugu extract above $0.1\ \text{nmol g}^{-1}$ (Extended Data Table 5). This difference could be a result of a more acidic pH of the fluids on Ryugu's

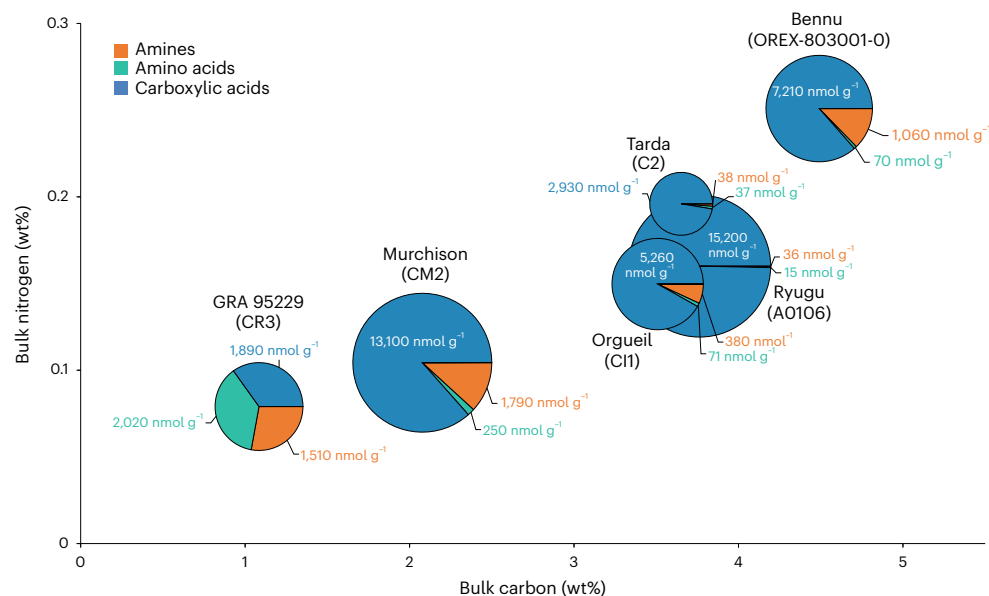


Fig. 5 | Distribution and total abundances of amines, amino acids and carboxylic acids in Benu (OREX-803001-0) compared with Ryugu (A0106) and selected CCs. Relative percentages of amines (orange), amino acids (green) and carboxylic acids (blue) are given in the individual pie charts with their overall size proportional to the total sum of the abundances of the three soluble organic compound classes. The pie charts are plotted on a bulk N versus C diagram to illustrate the total C and N abundance differences between the samples in weight percentage. The values for the total sum of the abundances of the molecules detected in each compound class are also given in nanomoles per gram for each pie slice. Although N-heterocycles were also quantified in Benu and Murchison, these data were excluded from this figure due to their low abundances relative

to the other compound classes and incomplete data for the other samples. The N-heterocycle abundance data for Benu, Murchison, Orgueil and Ryugu are included in Extended Data Table 6. Other water-soluble organic compounds such as aldehydes and ketones, hydroxy acids, cyanides and amides have been identified in CCs² but were not analysed in this study and are therefore also not included in the figure. The amine, amino acid and carboxylic acid data for Murchison and Benu are from this investigation (Extended Data Tables 2, 3 and 5). Previously published data from Ryugu²⁰ and GRA 95229 (ref. 15) are also shown. For Orgueil, published amine⁵⁸ and amino acid⁵⁹ data were used, whereas the carboxylic acid data are from this study (Extended Data Table 5). The data for Tarda from Extended Data Tables 2, 3 and 5 were also measured in this study.

parent body²¹ compared with Benu's, leading to their evaporation and/or more extensive aqueous alteration, ultimately decomposing or altering carboxylic acids²⁸. The structural diversity of carboxylic acids in Benu is consistent with an origin through stochastic low-temperature free radical reactions on interstellar dust grains²⁶. Isotopic analyses of carboxylic acids are needed to further constrain the abiotic origins of these molecules in Benu.

The total abundance of identified C₂ to C₆ protein and non-protein amino acids in the Benu hot-water extract (~70 nmol g⁻¹) was lower by a factor of 3.6 than that in Murchison but 4.7 times higher than in Ryugu extracts (Fig. 6 and Extended Data Table 3). Benu's total amino acid abundance resembles that of CI1 and some less altered CM2 and C2_{ung} chondrites (Fig. 6a). However, the amino acid distribution is dominated by glycine, with lower relative abundances of α-alanine, β-alanine, α-aminoisobutyric acid and isovaline compared with CCs (Fig. 6a). The high relative abundances of glycine and racemic mixtures of most α-amino acids suggest a formation by means of HCN polymerization and/or Strecker-cyanohydrin synthesis during aqueous alteration in Benu's parent body². However, alternate amino acid formation mechanisms^{2,29} are required to explain the formation of the β-, γ- and δ-amino acids observed in the hot-water extract (Extended Data Fig. 2 and Extended Data Table 3).

The low β-alanine/glycine ratio (~0.08) that we measured for Benu is unexpected based on trends observed in CCs (Fig. 6a) and Benu's CI-like elemental composition and mineralogy⁵. Higher β-alanine/glycine ratios, such as those found in type-1 chondrites and Ryugu samples (>2.7; Fig. 6a), align with extensive hydrothermal alteration, whereas the lower ratio in Benu is closer to the less aqueously altered type-2 chondrites (Fig. 6a).

Benu's amino acid distribution indicates a distinct chemical composition and/or lower-temperature aqueous alteration history of its

parent body compared with those of Ryugu and the aqueously altered CCs. Future analyses of the distribution and stable isotopic compositions of amino acids in Benu samples, including their precursors and related structures, will provide further insight into the formation and evolution of these prebiotic molecules.

The measurement of racemic isovaline (Fig. 6b) and other amino acids, within analytical error, was also unexpected (Extended Data Table 4). Based on the evidence for extensive water activity in Benu's parent body^{5,30,31}, we predicted that Benu samples would show some L-isovaline excess, following the empirical trend of higher extraterrestrial L-isovaline excesses in more aqueously altered CCs¹³. Furthermore, substantial L excesses in aspartic and glutamic acids (up to ~60%) measured in some lithologies of the Tagish Lake meteorite and attributed to amplification by crystallization of conglomerate-forming amino acids during parent body aqueous alteration³², were not observed in Benu aggregate either (Extended Data Table 4). The source of the meteoritic L-amino acid enrichments remains a mystery. At least for now, the lack of any amino acid enantiomeric excesses of confirmed extraterrestrial origin in the Benu material analysed here, as well as in samples from Ryugu^{20,27} and some lithologies of Tagish Lake and Tarda (Extended Data Table 4), challenges the hypothesis that the emergence of left-handed protein-based life on Earth was influenced by an early Solar System bias toward L-amino acids¹³.

The total abundance of N-heterocycles identified in Benu samples (~5 nmol g⁻¹; Extended Data Table 6) is 5–10 times higher than reported in Ryugu³³ and Orgueil³⁴. The elevated abundances and more complex distribution of N-heterocycles again may reflect a lower degree of hydrothermal alteration in Benu's parent body during organic synthesis compared with Ryugu's, which is consistent with trends that have been observed in aqueously altered CI and CM chondrites³⁴. However, the ratio of purines to pyrimidines is much lower

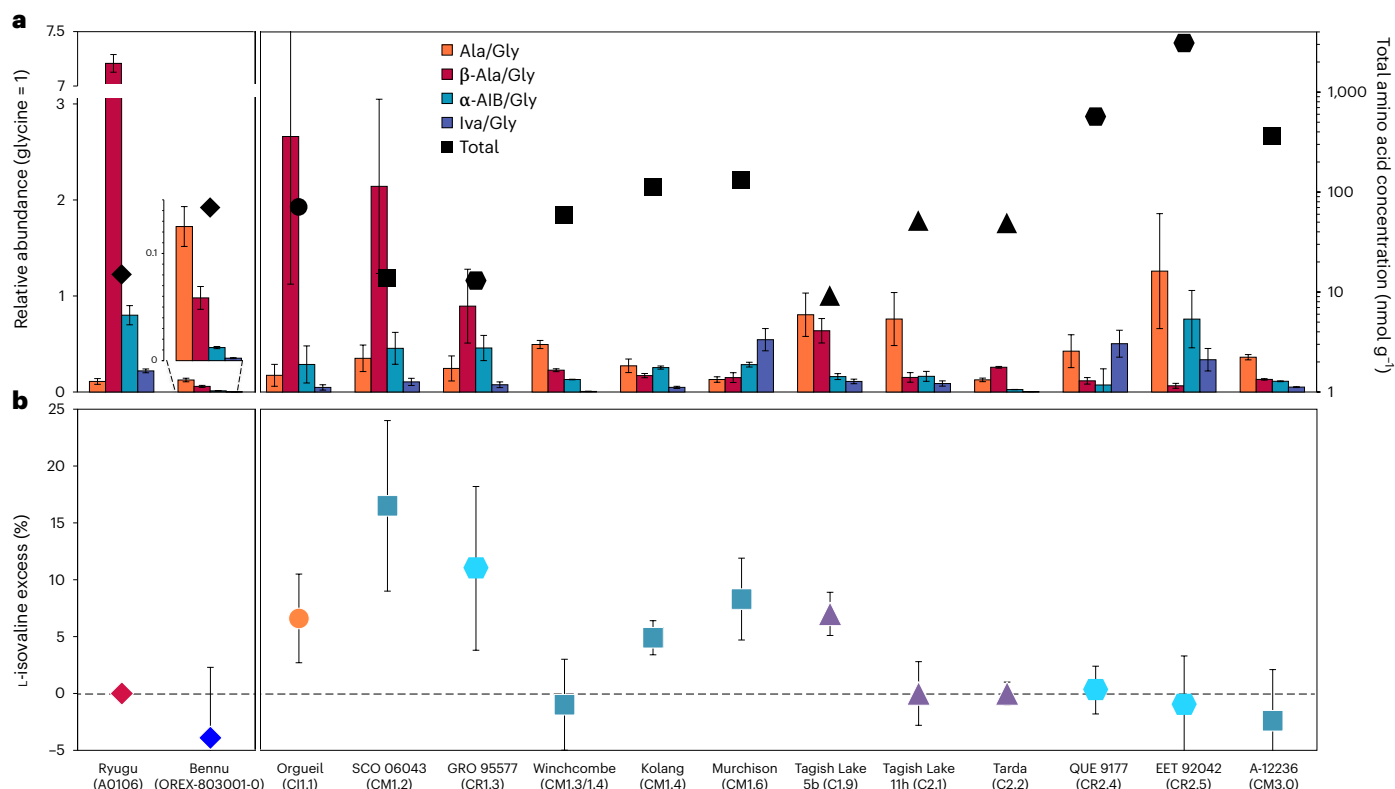


Fig. 6 | Relative abundances and total concentrations of amino acids and percentage of L-isovaline enantiomeric excesses measured by liquid chromatography mass spectrometry in Benu (OREX-803001-0) compared with Ryugu (A0106) and selected CCs. a, The relative molar abundances (left y axis, glycine = 1) of alanine (Ala), β-alanine (β-Ala), α-aminoisobutyric acid (α-AIB) and isovaline (Iva) are shown as coloured bars with uncertainties determined by standard error propagation of the absolute errors. The total concentrations of identified C₂ to C₆ amino acids in the 6 M HCl-hydrolysed, hot-water extracts of the samples are designated by the black data points (right y axis, logarithmic scale). **b,** L-isovaline excesses (%L_{ee} = %L – %D) and associated standard errors

were calculated from the average individual abundances of D- and L-isovaline in the same extracts. The amino acid data for Benu are the average values reported in Extended Data Tables 3 and 4. Published amino acid data from Ryugu, Orgueil, SCO 06043, GRO 95577, Murchison, Tagish Lake 5b and 11h, QUE 99177, EET 92042 and A-12236 are shown for comparison^{20,27,32,59,60}. The Winchcombe, Kolang and Tarda-RV data are newly published here. The CCs are ordered from least to most aqueously altered (right to left) as inferred from their petrologic type assignments shown in parentheses based on the abundance of H in OH/H₂O (ref. 56). The colours and symbols used were selected to differentiate between asteroids Benu and Ryugu, and the different CC groups (CI, CM, C₂_{ung} and CR).

in the Benu extract (0.55; Extended Data Table 6) than in Murchison (–2.8) and Orgueil (–1.1). This elevated abundance of pyrimidines over purines may be related to differences in the parent bodies' chemical composition, formation pathways and/or aqueous alteration histories. N-heterocycles can be readily synthesized from ammonia and formaldehyde, especially under alkaline conditions³⁵. Because pyrimidines are preferentially formed over purines in interstellar ice–analogue irradiation experiments³⁶, it is also possible that Benu's N-heterocycles and/or their chemical precursors were inherited from a cold molecular cloud environment. The unusual richness of N-heterocycles may be of relevance for prebiotic chemistry. Further studies of nucleobase chemistry in samples returned from Benu, from precursors to nucleic acids, are warranted.

Benu's origin and implications for prebiotic chemistry

The elevated volatile content, the large ¹⁵N enrichments of ammonia and other water-soluble N-containing molecules and the high abundance of N-rich isotopically anomalous organic matter³⁷ observed in the Benu samples suggest that the parent body accreted ices from a reservoir in the outer Solar System, where ammonia ice was stable (beyond Jupiter's current orbit). Dynamical simulations predict that Benu derived from a secondary parent body in the inner main belt (2.1–2.5 au) that broke up 730–1,550 Myr ago³⁸. The parent body may have originated in the outer Solar System, perhaps emplaced into the asteroid belt during giant-planet migrations, as has previously been

proposed for CI chondrites and Ryugu³⁹. Alternatively, ices may have migrated inward by means of pebble drift, a process where small, icy pebbles drift inward from the outer Solar System and accrete onto forming planetesimals in the asteroid belt. This mechanism would allow material from more distant, colder regions, where ammonia and other volatile ices are stable, to be incorporated into bodies forming closer to the Sun⁴⁰.

B-type asteroids such as Benu⁴¹, so named for their blue spectral slopes, and other small bodies that emit particles⁴² have been hypothesized⁴³ to be fragments of extinct comets sampling a continuum of objects, from dry planetesimals that formed close to the Sun to volatile-rich icy bodies that formed well beyond the water snow line. There is some evidence of low-temperature aqueous activity in comets, including the spectroscopic detection of hydrated minerals and carbonates in the impact ejecta of comet 9P/Tempel 1 by the Spitzer Space Telescope⁴⁴ and cubanite in samples from comet 81P/Wild⁴⁵. Nevertheless, the phyllosilicate-dominated bulk mineralogy of Benu samples⁵ and the spacecraft observations of metre-sized carbonate-rich veins³¹ on Benu both imply large-scale hydrothermal activity for millions of years that may not be consistent with a cometary parent body origin.

Alternatively, the presence of ammonium and carbonate salts, high organic carbon content and evidence of rock-fluid interactions observed in Ceres^{25,46,47} suggest that Benu may consist of fragments of a Ceres-like primitive icy body that experienced extensive low-temperature aqueous activity. Petrologic data from Benu samples

indicate that late-stage fluid in the parent body sequentially precipitated evaporite minerals, starting with Ca and Mg carbonates, progressing to phosphates, followed by Na carbonates and concluding with halides and sulfates⁴⁸. These minerals strongly imply alkaline pH, substantial concentrations of dissolved inorganic carbon and fluid temperatures below -55°C (ref. 48). This dynamically changing environment in Benu's parent body is likely to have fostered intricate interactions among brine fluid chemistry, soluble organics and freshly exposed mineral surfaces. High concentrations of ammonium salts in Benu's parent body could have created liquid brines at very low temperatures ($\text{NH}_3\text{--H}_2\text{O}$ eutectic of 176 K), and thus provided an aqueous environment for organic chemistry to continue even as the abundances of short-lived radionuclides responsible for internal heating were exhausted⁴⁹. For example, a suite of amino acids dominated by glycine and the purines adenine and guanine were produced in dilute NH_4CN kept at 195 K for 25 yr (ref. 50). Eutectic freezing, phyllosilicate catalysis, low-temperature template polymerization and Mg salts are employed in the laboratory polymerization of activated nucleotides⁵¹.

Additional analyses of Benu samples, coupled with laboratory analogue experiments and future sample return missions from a comet and Ceres, will be important to further understand the origin and evolution of prebiotic organic matter in Benu and potential chemical links between volatile-rich asteroids and primitive icy bodies. Regardless of their origins, asteroids such as Benu could have been a source of N-rich volatiles and compounds of biological importance, including ammonia, amino acids, nucleobases, phosphates and other chemical precursors that contributed to the prebiotic inventory that led to the emergence of life on Earth.

Methods

Before these investigations, validation of the analytical methods used in this study were performed on Murchison and Sutter's Mill as part of OSIRIS-REx sample analysis readiness tests^{52–54}.

Samples used in this investigation

The Benu aggregates studied (Supplementary Fig. 1) consisted of a mixture of mostly fine ($<100\text{ }\mu\text{m}$) to intermediate ($100\text{--}500\text{ }\mu\text{m}$) sized particles with some coarse ($>500\text{ }\mu\text{m}$) grains dominated by hydrous silicate minerals ($\sim 80\%$ phyllosilicates by volume) with lower abundances ($\leq 10\%$) of sulfides, magnetite, carbonates, anhydrous silicates (olivine and pyroxene) and other minor phases⁵. The Benu sample nomenclature as well as the detailed processing and analytical flow of the aggregate samples are summarized in Supplementary Table 1 and Supplementary Fig. 2.

Two aggregate samples (OREX-500002-0 and OREX-500005-0) that were included as part of the 'quick-look' (QL)^{5,12} analyses were removed from the avionics deck surface, weighed and then containerized under N_2 in the curation glovebox⁵⁵ at the NASA Johnson Space Center (JSC). OREX-500002-0 ($\sim 22\text{ mg}$) consisted primarily of dark fines and some intermediate-sized particles, with some bright and highly reflective particles, and numerous (>5) white fibres thought to be derived from the sample return capsule aluminized Kapton multilayer insulation filled with fibreglass. The sample was sealed under N_2 between two glass concavity slides and shipped from NASA JSC to the Carnegie Institution for Science (CIS). This sample was inspected under an optical microscope at CIS, and the fibres were physically removed from the sample with organically clean stainless-steel tweezers. A 1.1 mg subsample of the aggregate (OREX-501029-0) was then transferred from the concavity slide to a separate glass pyrolysis tube at CIS and carried by hand to the NASA Goddard Space Flight Center (GSFC) for targeted amino acid and N-heterocycle analyses using wet chemistry and pyGC-QqQ-MS (more detail about the method in the 'Coordinated analyses of organics in the aggregate samples' section below). The remaining $\sim 20\text{ mg}$ were further split into multiple subsamples for elemental and stable isotopic analyses of bulk carbon,

nitrogen and hydrogen, using an EA-IRMS instrument at CIS (details in the next section).

OREX-500005-0 consisted of mostly dark fines with an average grain size $<100\text{ }\mu\text{m}$, but with some particles up to $\sim 500\text{ }\mu\text{m}$. Some bright and highly reflective particles were also present in this aggregate sample; however, no fibres were observed. OREX-500005-0 ($\sim 88\text{ mg}$) was sealed under N_2 inside a glass vial with a Viton stopper and crimped aluminium lid. It was subsampled to obtain OREX-501006-0 ($<1\text{ mg}$) for coordinated optical and UV fluorescence microscopy and $\mu\text{-L}^3\text{MS}$ analyses at NASA JSC (see 'Coordinated analyses of organics in the aggregate samples' section for more detail about the methods below).

Bulk material from the touch-and-go sample acquisition mechanism (TAGSAM) was subsampled to obtain TAGSAM aggregate (TA) samples OREX-800031-0 ($\sim 52\text{ mg}$) and OREX-800044-0 ($\sim 109\text{ mg}$). OREX-800031-0 was shipped from JSC to GSFC in a glass concavity slide (Supplementary Fig. 1) that was hermetically sealed under high purity N_2 inside an Eagle Stainless container. The container was opened inside an ISO 5 HEPA-filtered laminar flow hood housed in an ISO-7 white room and the aggregate sample was subsampled and distributed for multiple analyses following a coordinated analysis scheme (Supplementary Fig. 2). A similar mass of a powdered sample of the CM2 Murchison from the University of Illinois, Chicago, and a powdered sample of fused silica (FS-120, HP Technical Ceramics) that had been previously ashed at 500°C in air overnight to remove organic contaminants were also processed in parallel with the Benu OREX-800031-0 aggregate sample. Procedural solvent blanks were also processed in parallel and analysed. OREX-800044-0 was shipped from JSC to Hokkaido University in Japan in a glass concavity slide (Supplementary Fig. 1) that was hermetically sealed under high purity N_2 inside an Eagle Stainless container. It was further subsampled in a glass concavity slide to OREX-800044-101 (17.75 mg) and shipped to Kyushu University in Japan.

Bulk C, N and H contents and their isotopic compositions

The elemental abundances of carbon (C, wt%), nitrogen (N, wt%) and hydrogen (H, wt%) and their isotopic compositions $\delta^{13}\text{C}$, in parts per thousand relative to the Vienna Pee Dee Belemnite, $\delta^{15}\text{N}$, in parts per thousand relative to Earth atmospheric nitrogen, and δD , in parts per thousand relative to the Vienna Standard Mean Ocean Water isotope reference, were analysed in subsamples of OREX-500002-0 and OREX-803007-0 and in a sample of the Murchison meteorite processed in parallel with OREX-803007-0 at GSFC after extraction in water at 100°C for 24 h. These measurements were made with: (1) a Thermo Scientific Delta V^{plus} isotope ratio mass spectrometer (IRMS) connected to a Carlo Erba elemental analyser (EA) by means of a ConFlo III interface for C and N analyses; and (2) a Thermo Scientific Delta Q IRMS connected to a Thermo Finnigan Thermal Conversion elemental analyser by means of a ConFlo IV interface for H analyses using previously described methods⁵⁶. The subsample masses used for H and C + N analyses were $\sim 1\text{--}1.5\text{ mg}$ and 5.5 mg , respectively. Subsamples were placed in an Ar-flushed glovebox and heated to 120°C for 48 h to reduce the amount of adsorbed atmospheric water before analysis (Supplementary Table 2). The reported uncertainties for the elemental and isotopic analyses correspond to a 1 σ standard deviation, which was determined based on either replicate analyses of standards or analyses of at least two aliquots of individual samples, with the larger error reported.

Small aliquots ($\sim 2.5\%$ of total extracted volume) of the hot-water extracts from TA OREX-803001-0 (designated split OREX-803001-112) and the parallel processed Murchison meteorite were transferred to separate tin capsules, acidified with $2\text{ }\mu\text{l}$ 6 M HCl, and then evaporated to dryness under vacuum at room temperature in a Labconco CentriVap Concentrator at GSFC. The capsules were crimped and analysed in series along with appropriate procedural blanks and standards using the nano EA-IRMS instrument at Pennsylvania State University (PSU) to determine the total C and N abundances as well as the $\delta^{13}\text{C}$ and

$\delta^{15}\text{N}$ values following published methods⁵⁷. These analyses were performed after verification of the analytical method with the predicted concentration of ammonia in the TA water extract and corresponding volume of NH_4OH . The nano EA-IRMS system at PSU employed a Flash IRMS elemental analyser that was coupled by means of a ConFlo IV Universal Interface to a Thermo Scientific Delta V^{plus} IRMS with a universal triple collector. Additional description of the nano EA-IRMS data processing methods and mass balance calculations can be found in the Supplementary Information.

Coordinated analyses of organics in the aggregate samples

OREX-800031-0 was subsampled for multiple analyses (Supplementary Fig. 2). OREX-803007-0 (23.6 mg) was allocated for bulk H, C and N measurements using EA-IRMS analyses at CIS. OREX-803006-0 (3.3 mg) was allocated for non-targeted molecular profiling of soluble organics in a methanol extract using FTICR-MS at Helmholtz-Zentrum in Munich, Germany. OREX-803004-0 (1.0 mg) was heated at 85 °C for 1.5 h in a sealed pyrolysis tube containing a 5 μl solution (4:1 v/v) of *N*-(*tert*-butyldimethylsilyl)-*N*-methyl-trifluoroacetamide and *N,N*-dimethylformamide and the sample was then analysed directly for the *N*-(*tert*-butyldimethylsilyl)-*N*-methyl-trifluoroacetamide derivatives of amino acids and N-heterocycles by pyGC-QqQ-MS at NASA GSFC. The remaining mass of OREX-803001-0 (25.6 mg) was flame-sealed in a glass ampoule with 1 ml Milli-Q ultrapure water (18.2 M Ω , <3 ppb total organic C) and heated at 100 °C for 24 h.

After water extraction, OREX-803001-0 was centrifuged (5 min at 3,000 rpm), and the water supernatant was separated from the solid residue. Some of the solid residue (OREX-803001-103, 22.9 mg) after water extraction was dried under vacuum at room temperature and sent to CIS for bulk H, C and N measurements. 17.5% of the OREX-803001-0 hot-water extract was analysed directly for free ammonia, hydrazine, aliphatic amines and protein amino acids. These analyses were performed by AccQ-Tag derivatization and liquid chromatography with UV fluorescence detection and either time-of-flight mass spectrometry (LC-FD/ToF-MS) or triple quadrupole mass spectrometry.

Approximately 2.5% of the OREX-803001-0 water extract was analysed by nano EA-IRMS for total C and N at PSU, as previously described. The remaining 80% of the OREX-803001-0 water extract was split equally, with 40% of the water extract desalted by cation exchange chromatography followed by *o*-phthalaldehyde/*N*-acetyl-L-cysteine (OPA/NAC) derivatization and analysis using both LC-FD/ToF-MS and liquid chromatography with UV fluorescence detection and high-resolution mass spectrometry (LC-FD/HRMS) to determine the free amino acid abundances in the extract. The other 40% was dried, acid-hydrolysed under 6 M HCl vapour at 150 °C for 3 h and then desalted to determine the average total (free + bound) amino acid abundances using both LC-FD/ToF-MS and LC-FD/HRMS. We also measured the distribution and abundances of the 2-pentanol derivatives of free mono- and dicarboxylic acids in the water wash collected during desalting (cation exchange) of the non-hydrolysed water extract of Bennu (OREX-803001-0) using GC-QqQ-MS.

A separate 17.75 mg aggregate sample (OREX-800044-101), subsampled from Bennu OREX-800044-0, was extracted in HCl (Tama Chemicals Co., Ltd.) and analysed for N-heterocycles using HPLC/ESI-HRMS at Kyushu University in Japan. A 14.4 mg ashed sample of sea sand (FUJIFILM Wako Pure Chemical Corporation; 30–50 mesh) was used as a processing blank for OREX-800044-101. Procedural solvent blanks were also processed in parallel and analysed.

A small subsample (<1 mg) of the QL aggregate (OREX-501006-0) was prepared at NASA JSC for coordinated analysis by optical and UV fluorescence microscopy and $\mu\text{-L}^2\text{MS}$. Approximately a dozen grains of the QL aggregate were transferred to an infrared grade potassium bromide (KBr) window and gently pressed into the KBr surface using an optical grade sapphire window. The sample mount was imaged optically and under UV fluorescence using an Olympus BX-60 microscope

equipped with a tungsten halogen and Hg-arc illumination sources. Native fluorescence images were obtained using 330–385 nm excitation and 420 nm long-pass emission filters. After optical and UV fluorescence imaging, the sample was transferred to a $\mu\text{-L}^2\text{MS}$ instrument and in situ mass spectra were acquired at a 5 μm spatial resolution using an infrared laser (CO_2 ; 10.6 mm) for desorption, a vacuum ultraviolet laser (Nd:YAG 9th harmonic; 118 nm) for photoionization and a reflectron time-of-flight mass spectrometer for mass analysis. Additional details of the imaging and $\mu\text{-L}^2\text{MS}$ analyses can be found in the Supplementary Information.

Data availability

The instrument data supporting the experimental results in this study are available at <https://astromat.org> at the DOIs given in Supplementary Table 14 and/or within the manuscript and its Supplementary Information. Source data are provided with this paper.

References

- Pearson, V. K. et al. Carbon and nitrogen in carbonaceous chondrites: elemental abundances and stable isotopic compositions. *Meteorit. Planet. Sci.* **41**, 1899–1918 (2006).
- Glavin, D. P. et al. in *Primitive Meteorites and Asteroids* (ed. Abreu, N.) 205–271 (Elsevier, 2018).
- DeMeo, F. E. & Carry, B. Solar system evolution from compositional mapping of the asteroid belt. *Nature* **505**, 629–634 (2014).
- Lee, M. R. et al. CM carbonaceous chondrite falls and their terrestrial alteration. *Meteorit. Planet. Sci.* **56**, 34–48 (2021).
- Lauretta, D. S. et al. Asteroid (101955) Bennu in the laboratory: properties of the sample collected by OSIRIS-REx. *Meteorit. Planet. Sci.* **59**, 2453–2486 (2024).
- Lauretta, D. S. et al. OSIRIS-REx: sample return from asteroid (101955) Bennu. *Space Sci. Rev.* **212**, 925–984 (2017).
- Lauretta, D. S. et al. The unexpected surface of asteroid (101955) Bennu. *Nature* **568**, 55–60 (2019).
- Simon, A. A. et al. Widespread carbon-bearing materials on near-Earth asteroid (101955) Bennu. *Science* <https://doi.org/10.1126/science.abc3522> (2020).
- Kaplan, H. H. et al. Composition of organics on asteroid (101955) Bennu. *Astron. Astrophys.* **653**, L1 (2021).
- Lauretta, D. S. et al. Spacecraft sample collection and subsurface excavation of asteroid (101955) Bennu. *Science* **377**, 285–291 (2022).
- DellaGiustina, D. N. et al. Variations in color and reflectance on the surface of asteroid (101955) Bennu. *Science* **370**, eabc3660 (2020).
- Lauretta, D. S., Connolly Jr, H. C., Grossman, J. N. & Polit, A. T. OSIRIS-REx sample analysis plan—revision 3.0. Preprint at <https://arxiv.org/abs/2308.11794> (2023).
- Glavin, D. P., Burton, A. S., Elsila, J. E., Aponte, J. C. & Dworkin, J. P. The search for chiral asymmetry as a potential biosignature in our solar system. *Chem. Rev.* **120**, 4660–4689 (2020).
- Bierhaus, E. B. et al. The OSIRIS-REx spacecraft and the touch-and-go sample acquisition mechanism (TAGSAM). *Space Sci. Rev.* **214**, 1–46 (2018).
- Pizzarello, S. et al. Abundant ammonia in primitive asteroids and the case for a possible exobiology. *Proc. Natl Acad. Sci. USA* **108**, 4303–4306 (2011).
- Pizzarello, S. & Williams, L. B. Ammonia in the early Solar System: an account from carbonaceous chondrites. *Astrophys. J.* <https://doi.org/10.1088/0004-637X/749/2/161> (2012).
- Schmitt-Kopplin, P. Z. et al. High molecular diversity of extraterrestrial organic matter in Murchison meteorite revealed 40 years after its fall. *Proc. Natl Acad. Sci. USA* **107**, 2763–2768 (2010).

18. Hoefs, J. *Stable Isotope Geochemistry* 54–57 (Springer-Verlag, 2009).
19. Alexander, C. M. O'D. et al. The provenances of asteroids, and their contributions to the volatile inventories of the terrestrial planets. *Science* **337**, 721–723 (2012).
20. Naraoka, H. et al. Soluble organic molecules in samples of the carbonaceous asteroid (162173) Ryugu. *Science* **379**, eabn9033 (2023).
21. Yoshimura, T. et al. Chemical evolution of primordial salts and organic sulfur molecules in the asteroid 162173 Ryugu. *Nat. Commun.* **14**, 5284 (2023).
22. Laize-G  n  rat, L. et al. Nitrogen in the Orgueil meteorite: abundant ammonium among other reservoirs of variable isotopic compositions. *Geochim. Cosmochim. Acta* **387**, 111–129 (2024).
23. Altwegg, K. et al. Evidence of ammonium salts in comet 67P as explanation for the nitrogen depletion in cometary comae. *Nat. Astron.* **4**, 533–540 (2020).
24. Poch, O. et al. Ammonium salts are a reservoir of nitrogen on a cometary nucleus and possibly on some asteroids. *Science* **367**, eaaw7462 (2020).
25. De Sanctis, M. C. et al. Ammoniated phyllosilicates with a likely outer Solar System origin on (1) Ceres. *Nature* **528**, 241–244 (2015).
26. Aponte, J. C., Woodward, H. K., Abreu, N. M., Elsila, J. E. & Dworkin, J. P. Molecular distribution, ¹³C-isotope, and enantiomeric compositions of carbonaceous chondrite monocarboxylic acids. *Meteorit. Planet. Sci.* **54**, 415–430 (2019).
27. Parker, E. T. et al. Extraterrestrial amino acids and amines identified in asteroid Ryugu samples returned by the Hayabusa2 mission. *Geochim. Cosmochim. Acta* **347**, 42–57 (2023).
28. Takano, Y. et al. Primordial aqueous alteration recorded in water-soluble organic molecules from the carbonaceous asteroid (162173) Ryugu. *Nat. Commun.* **15**, 5708 (2024).
29. Koga, T. & Naraoka, H. Synthesis of amino acids from aldehydes and ammonia: implications for organic reactions in carbonaceous chondrite parent bodies. *ACS Earth Space Chem.* **6**, 1311–1320 (2022).
30. Hamilton, V. E. et al. Evidence for widespread hydrated minerals on asteroid (101955) Bennu. *Nat. Astron.* **3**, 332–340 (2019).
31. Kaplan, H. H. et al. Bright carbonate veins on asteroid (101955) Bennu: implications for aqueous alteration history. *Science* **370**, eabc3557 (2020).
32. Glavin, D. P. et al. Unusual non-terrestrial L-proteinogenic amino acid excesses in the Tagish Lake meteorite. *Meteorit. Planet. Sci.* **47**, 1347–1364 (2012).
33. Oba, Y. et al. Uracil in the carbonaceous asteroid (162173) Ryugu. *Nat. Commun.* **14**, 1292 (2023).
34. Callahan, M. P. et al. Carbonaceous meteorites contain a wide range of extraterrestrial nucleobases. *Proc. Natl Acad. Sci. USA* **108**, 13995–13998 (2011).
35. Naraoka, H. et al. Molecular evolution of N-containing cyclic compounds in the parent body of the Murchison meteorite. *ACS Earth Space Chem.* **1**, 540–550 (2017).
36. Oba, Y. et al. Identifying the wide diversity of extraterrestrial purine and pyrimidine nucleobases in carbonaceous meteorites. *Nat. Commun.* **13**, 2008 (2022).
37. Nguyen, A. N. et al. N-rich isotopically anomalous nanoglobules and organic matter in Bennu. In *86th Annual Meeting of the Meteoritical Society* <https://www.hou.usra.edu/meetings/metsoc2024/pdf/6446.pdf> (2024).
38. Walsh, K. J. et al. Numerical simulations suggest asteroids (101955) Bennu and (162173) Ryugu are likely second or later generation rubble piles. *Nat. Commun.* **15**, 5653 (2024).
39. Hopp, T. et al. Ryugu's nucleosynthetic heritage from the outskirts of the Solar System. *Sci. Adv.* **8**, eadd8141 (2022).
40. Booth, R. A. & Ilee, J. D. Planet-forming material in a protoplanetary disk: the interplay between chemical evolution and pebble drift. *Mon. Not. R. Astron. Soc.* **487**, 3998–4011 (2019).
41. Lauretta, D. S. et al. Episodes of particle ejection from the surface of the active asteroid (101955) Bennu. *Science* **366**, eaay3544 (2019).
42. Fernandez, Y. R., McFadden, L. A., Lisse, C. M., Helin, E. F. & Chamberlin, A. B. Analysis of POSS images of comet–asteroid transition object 107P/1949 W1 (Wilson–Harrington). *Icarus* **128**, 114–126 (1997).
43. Nuth, J. A. III et al. Volatile-rich asteroids in the inner Solar System. *Planet. Sci. J.* **1**, 82 (2020).
44. Lisse, C. M. et al. Spitzer spectral observations of the Deep Impact ejecta. *Science* **313**, 635–640 (2006).
45. Berger, E. L., Zega, T. J., Keller, L. P. & Lauretta, D. S. Evidence for aqueous activity on comet 81P/Wild 2 from sulfide mineral assemblages in stardust samples and CI chondrites. *Geochim. Cosmochim. Acta* **75**, 3501–3513 (2011).
46. Castillo-Rogez, J. et al. Insights into Ceres's evolution from surface composition. *Meteorit. Planet. Sci.* **53**, 1820–1843 (2018).
47. Marchi, S. et al. An aqueously altered carbon-rich Ceres. *Nat. Astron.* **3**, 140–145 (2019).
48. McCoy, T. J. et al. An evaporite sequence from ancient brine recorded in Bennu samples. *Nature* <https://doi.org/10.1038/s41586-024-08495-6> (2025).
49. Dyl, K. A. et al. Early solar system hydrothermal activity in chondritic asteroids on 1–10-year timescales. *Proc. Natl Acad. Sci. USA* **109**, 18306–18311 (2012).
50. Levy, M., Miller, S. L., Brinton, K. & Bada, J. L. Prebiotic synthesis of adenine and amino acids under Europa-like conditions. *Icarus* **145**, 609–613 (2000).
51. Szostak, J. W. The narrow road to the deep past: in search of the chemistry of the origin of life. *Angew. Chem. Int. Ed. Engl.* **56**, 10959–11271 (2017).
52. Cody, G. D. et al. Testing the effect of x-ray computed tomography on chondritic insoluble organic matter and exploring parent body molecular evolution. *Meteorit. Planet. Sci.* **59**, 3–22 (2024).
53. Nguyen, A. N. et al. Micro- and nanoscale studies of insoluble organic matter and C-rich presolar 2 grains in Murchison and Sutteras Mill in preparation for Bennu sample analysis. *Meteorit. Planet. Sci.* **59**, 2831–2850 (2024).
54. Glavin, D. P. et al. Investigating the impact of x-ray computed tomography imaging on soluble organic matter in the Murchison meteorite: implications for Bennu sample analyses. *Meteorit. Planet. Sci.* **59**, 105–133 (2024).
55. Righter, K. et al. Curation planning and facilities for asteroid Bennu samples returned by the OSIRIS-REx mission. *Meteorit. Planet. Sci.* **58**, 572–590 (2023).
56. Alexander, C. M. O'D., Howard, K., Bowden, R. & Fogel, M. L. The classification of CM and CR chondrites using bulk H, C and N abundances and isotopic compositions. *Geochim. Cosmochim. Acta* **123**, 244–260 (2013).
57. Baczynski, A. A., Brodie, C. R., Kracht, O. & Freeman, K. H. Sequential measurement of ¹³C, ¹⁵N, and ³⁴S isotopic composition on nanomolar quantities of carbon, nitrogen, and sulfur using nano-elemental/isotope ratio mass spectrometry. *Rapid Commun. Mass Spectrom.* **37**, e9444 (2023).
58. Aponte, J. C., Dworkin, J. P. & Elsila, J. E. Indigenous aliphatic amines in the aqueously altered Orgueil meteorite. *Meteorit. Planet. Sci.* **50**, 1733–1749 (2015).
59. Glavin, D. P. et al. The effects of parent body processes on amino acids in carbonaceous chondrites. *Meteorit. Planet. Sci.* **45**, 1948–1972 (2010).

60. Glavin, D. P. et al. Abundant extraterrestrial amino acids in the primitive CM carbonaceous chondrite Asuka 12236. *Meteorit. Planet. Sci.* **55**, 1979–2006 (2020).
61. Alexander, C. M. O'D. et al. Elemental, isotopic, and structural changes in Tagish Lake insoluble organic matter produced by parent body processes. *Meteorit. Planet. Sci.* **49**, 503–525 (2014).
62. Burton, A. S., Grunsfeld, S., Elsila, J. E., Glavin, D. P. & Dworkin, J. P. The effects of parent-body hydrothermal heating on amino acid abundances in CI-like chondrites. *Polar Sci.* **8**, 255–263 (2014).
63. Koga, T., Takano, Y., Oba, Y., Naraoka, H. & Ohkouchi, N. Abundant extraterrestrial purine nucleobases in the Murchison meteorite: implications for a unified mechanism for purine synthesis in carbonaceous chondrite parent bodies. *Geochim. Cosmochim. Acta* **365**, 253–265 (2024).
64. Stoks, P. G. & Schwartz, A. W. Uracil in carbonaceous meteorites. *Nature* **282**, 709–710 (1979).

Acknowledgements

We are grateful to the entire OSIRIS-REx team for making the return of samples from asteroid Bennu possible. We thank the Astromaterials Acquisition and Curation Office, part of the Astromaterials Research and Exploration Science Division at NASA Johnson Space Center, for their efforts in sample return capsule recovery, preliminary examination and long-term curation. We also greatly appreciate support from the OSIRIS-REx Sample Analysis Micro Information System team. We are grateful to R. Vargas (meteorite hunter) for providing a sample of the C2 ungrouped Tarda meteorite, L. Garvie (Arizona State University) for providing the CM1/2 Kolang meteorite (sample ASU 2147) and D. Hill (Lunar and Planetary Laboratory, University of Arizona) for allocating the CM2 Winchcombe meteorite (sample UA2925,12). We also thank R. Minard and the Clifford N. Matthews research group at the University of Illinois, Chicago, for providing the Murchison meteorite used in this investigation. We also appreciate the careful review of the manuscript by C.W.V. Wolner. This material is based upon work supported by NASA award no. NNH09ZDA0070 and under contract no. NNM10AA11C issued through the New Frontiers Program. Z.G. and G.D. are supported by NASA OSIRIS-REx Sample Analysis Participating Scientist Program (ORSA-PSP) award. no. 80NSSC22K1692. Y.H., E.S. and B.K. are supported by NASA ORSA-PSP award no. 80NSSC22K1691. K.H.F., A.A.B., C.H.H., O.M.M. and M.M. are supported by NASA ORSA-PSP award no. 80NSSC22K1690. Work at the Molecular Foundry and Advanced Light Source was supported by the Office of Science, Office of Basic Energy Sciences, of the US Department of Energy under contract no. DE-AC02-05CH11231. P.S.-K. and M.L. were funded by the German Research Foundation—project-ID 364653263—TRR 235 (CRC 235) and project-ID 521256690—TRR 392/1 2024 (CRC 392/1 B2). Y.O. is supported by the Japan Society for the Promotion of Science under KAKENHI grant nos 21H04501 and 23H03980. D.I.F., C.M.O'D.A. and G.C. are supported by the Emerging Worlds grant nos 80NSSC20K0344 and 80NSSC21K0654, and D.I.F. is also funded through Exobiology grant no. 80NSSC21K0485. P.R.H. and Y.Z. acknowledge support by the TAWANI Foundation. A.H.C., D.N.S., F.S., H.L.M. and K.K.F. are supported by the Center for Research and Exploration in Space Science and Technology II cooperative agreement with NASA and the University of Maryland, Baltimore County, under award no. 80GSFC24M0006. A.E.H. is supported by 21-ORSAPS21_2-0009. The Jet Propulsion Laboratory is operated by the California Institute of Technology under

contract with NASA (contract no. 80NM0018D0004). This research used resources of the Advanced Light Source, a U.S. DOE Office of Science User Facility under contract no. DE-AC02-05CH11231.

Author contributions

D.P.G. and J.P.D. contributed equally. D.P.G., J.P.D., J.C.A., H.L.M., A.M., E.T.P., Y.O., T.K., D.I.F., C.M.O'D.A., P.S.-K., A.B., K.H.F., Z.G., M.A.M., G.D., P.H., S.J.C., A.N.N., K.L.T.-K., S.A.S., H.C.C. and D.S.L. conceptualized the study. D.P.G., J.P.D., J.C.A., H.L.M., A.M., E.T.P., Y.O., T.K., D.I.F., C.M.O'D.A., G.C., P.S.-K., M.L., P.C., A.S., T.G., B.M.G., A.B., K.H.F., Z.G., M.A.M., G.D., P.H., S.J.C., A.N.N., P.H., F.S., D.N.S., K.L.T.-K., S.A.S., E.B. and A.S.B. were responsible for the methodology and the investigation. The original draft was written by D.P.G., J.P.D., J.C.A., H.L.M., A.M., E.T.P., Y.O., T.K., P.S.-K., D.I.F., C.M.O'D.A., A.B., K.H.F., Z.G., M.A.M., G.D., S.J.C. and A.N.N. All coauthors reviewed and edited the manuscript.

Competing interests

The authors declare no competing interests.

Additional information

Extended data is available for this paper at <https://doi.org/10.1038/s41550-024-02472-9>.

Supplementary information The online version contains supplementary material available at <https://doi.org/10.1038/s41550-024-02472-9>.

Correspondence and requests for materials should be addressed to Daniel P. Glavin.





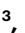

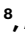


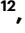

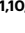
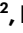


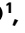




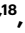
Peer review information *Nature Astronomy* thanks Zita Martins, Larry Nittler and the other, anonymous, reviewer(s) for their contribution to the peer review of this work.

Reprints and permissions information is available at www.nature.com/reprints.

Publisher's note Springer Nature remains neutral with regard to jurisdictional claims in published maps and institutional affiliations.

Open Access This article is licensed under a Creative Commons Attribution 4.0 International License, which permits use, sharing, adaptation, distribution and reproduction in any medium or format, as long as you give appropriate credit to the original author(s) and the source, provide a link to the Creative Commons licence, and indicate if changes were made. The images or other third party material in this article are included in the article's Creative Commons licence, unless indicated otherwise in a credit line to the material. If material is not included in the article's Creative Commons licence and your intended use is not permitted by statutory regulation or exceeds the permitted use, you will need to obtain permission directly from the copyright holder. To view a copy of this licence, visit <http://creativecommons.org/licenses/by/4.0/>.

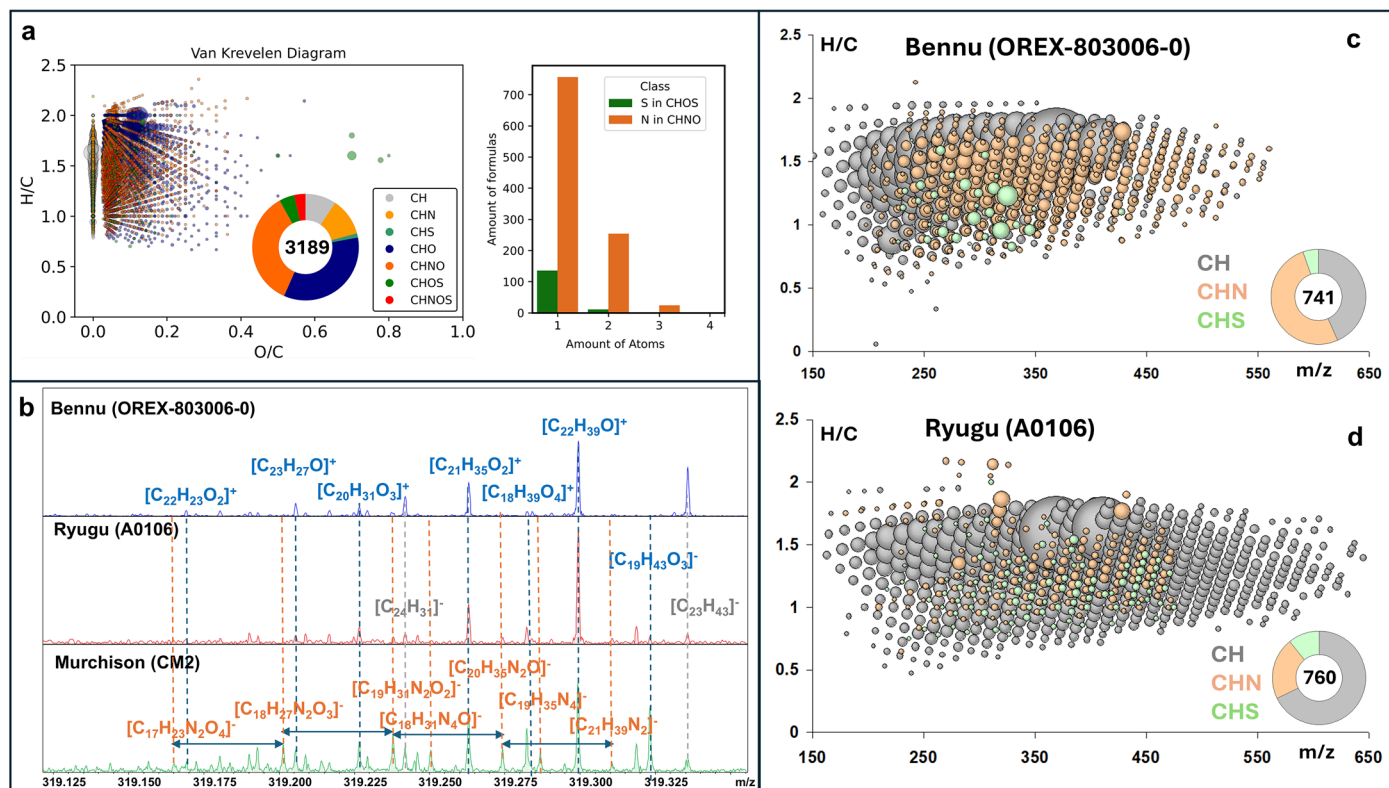
This is a U.S. Government work and not under copyright protection in the US; foreign copyright protection may apply 2025

Daniel P. Glavin ^{1,37}✉, **Jason P. Dworkin** ^{1,37}, **Conel M. O'D. Alexander** ², **José C. Aponte** ¹, **Allison A. Baczynski** ³, **Jessica J. Barnes** ⁴, **Hans A. Bechtel**⁵, **Eve L. Berger**⁶, **Aaron S. Burton** ⁷, **Paola Caselli** ⁸, **Angela H. Chung** ^{1,9,10}, **Simon J. Clemett**^{6,11}, **George D. Cody**², **Gerardo Dominguez** ¹², **Jamie E. Elsila** ¹, **Kendra K. Farnsworth** ^{1,10,13}, **Dionysis I. Foustoukos** ², **Katherine H. Freeman**³, **Yoshihiro Furukawa** ¹⁴, **Zack Gainsforth** ¹⁵, **Heather V. Graham** ¹, **Tommaso Grassi** ⁸, **Barbara Michela Giuliano** ⁸, **Victoria E. Hamilton** ¹⁶, **Pierre Haenecour** ⁴, **Philipp R. Heck** ^{17,18},

Amy E. Hofmann¹⁹, Christopher H. House³, Yongsong Huang²⁰, Hannah H. Kaplan¹, Lindsay P. Keller⁶, Bumsoo Kim^{6,20,21}, Toshiki Koga²², Michael Liss^{23,24}, Hannah L. McLain^{1,9,10}, Matthew A. Marcus⁵, Mila Matney³, Timothy J. McCoy²⁵, Ophélie M. McIntosh³, Angel Mojarro^{1,26}, Hiroshi Naraoka²⁷, Ann N. Nguyen⁶, Michel Nuevo²⁸, Joseph A. Nuth III¹, Yasuhiro Oba²⁹, Eric T. Parker¹, Tanya S. Peretyazhko^{6,21}, Scott A. Sandford²⁸, Ewerton Santos²⁰, Philippe Schmitt-Kopplin^{8,23,24}, Frederic Seguin^{1,10}, Danielle N. Simkus^{1,9,10}, Anique Shahid^{8,30}, Yoshinori Takano^{22,31}, Kathie L. Thomas-Keprta^{6,32}, Havishk Tripathi^{1,33}, Gabriella Weiss^{1,13}, Yuke Zheng^{17,18}, Nicole G. Lunning⁶, Kevin Richter³⁴, Harold C. Connolly Jr.^{4,35,36} & Dante S. Lauretta⁴

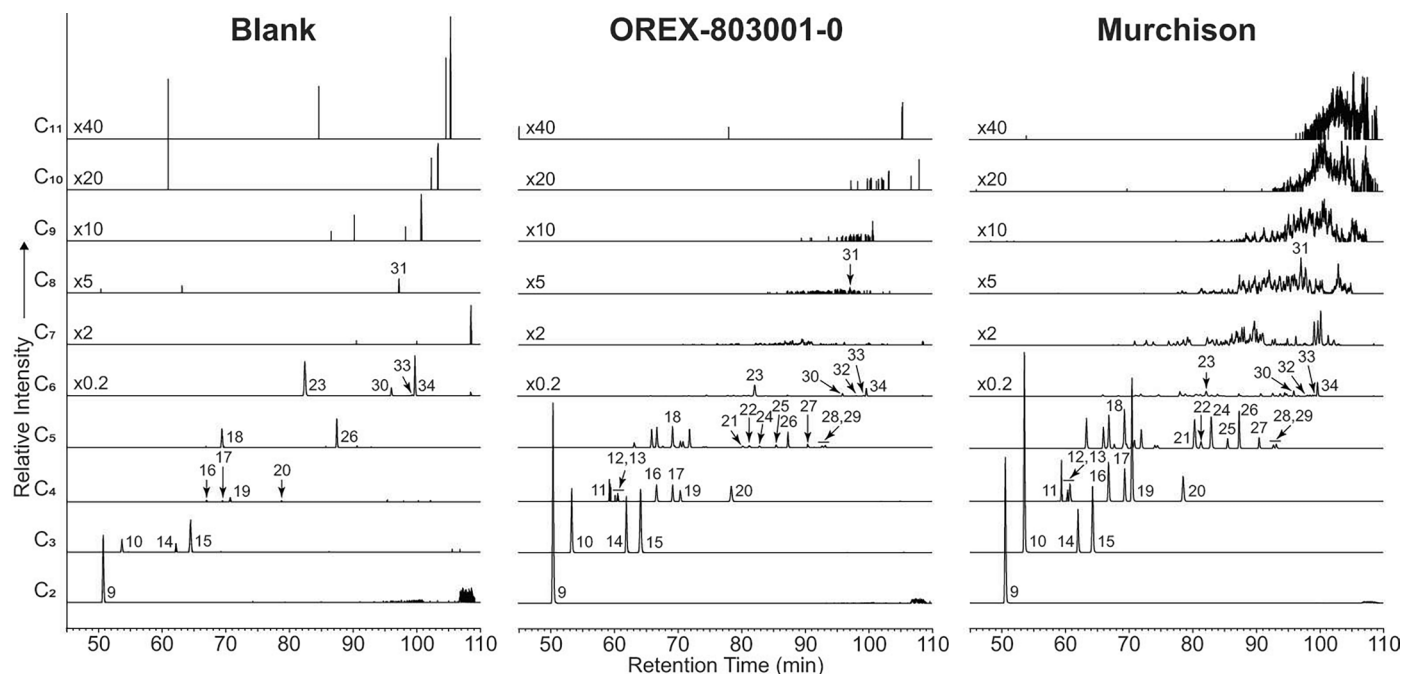
¹Solar System Exploration Division, NASA Goddard Space Flight Center (GSFC), Greenbelt, MD, USA. ²Earth and Planets Laboratory, Carnegie Institution for Science, Washington, DC, USA. ³Department of Geosciences, Pennsylvania State University, University Park, PA, USA. ⁴Lunar and Planetary Laboratory, University of Arizona, Tucson, AZ, USA. ⁵Lawrence Berkeley National Laboratory, Berkeley, CA, USA. ⁶Astromaterials Research and Exploration Science Division, NASA Johnson Space Center, Houston, TX, USA. ⁷NASA Headquarters, Washington, DC, USA. ⁸Center for Astrochemical Studies, Max Planck Institute for Extraterrestrial Physics, Garching, Germany. ⁹Department of Chemistry, Catholic University of America, Washington, DC, USA. ¹⁰Center for Research and Exploration in Space Science and Technology, NASA GSFC, Greenbelt, MD, USA. ¹¹ERC, Inc., JETS/Jacobs, Houston, TX, USA. ¹²California State University San Marcos, San Marcos, CA, USA. ¹³Center for Space Sciences and Technology, University of Maryland Baltimore County, Baltimore, MD, USA. ¹⁴Department of Earth Science, Tohoku University, Sendai, Japan. ¹⁵Space Science Laboratory, University of California, Berkeley, CA, USA. ¹⁶Southwest Research Institute, Boulder, CO, USA. ¹⁷Robert A. Pritzker Center for Meteoritics and Polar Studies, Negaunee Integrative Research Center, Field Museum of Natural History, Chicago, IL, USA. ¹⁸Department of the Geophysical Sciences, University of Chicago, Chicago, IL, USA. ¹⁹Jet Propulsion Laboratory, California Institute of Technology, Pasadena, CA, USA. ²⁰Department of Earth, Environmental, and Planetary Science, Brown University, Providence, RI, USA. ²¹Amentum, JSC Engineering and Technical Support (JETSII) Contract, NASA Johnson Space Center, Houston, TX, USA. ²²Biogeochemistry Research Center, Japan Agency for Marine-Earth Science and Technology (JAMSTEC), Natsushima, Yokosuka, Japan. ²³Technical University Munich, Freising, Germany. ²⁴Research Unit Analytical Biogeochemistry, Helmholtz Munich, Neuherberg, Germany. ²⁵National Museum of Natural History, Smithsonian Institution, Washington, DC, USA. ²⁶Oak Ridge Associated Universities, Oak Ridge, TN, USA. ²⁷Department of Earth and Planetary Sciences, Kyushu University, Fukuoka, Japan. ²⁸NASA Ames Research Center, Moffett Field, CA, USA. ²⁹Institute of Low Temperature Science, Hokkaido University, N19W8 Kita-ku, Sapporo, Japan. ³⁰Department of Physics, Technische Universität München, Muenchen, Germany. ³¹Institute for Advanced Biosciences, Keio University, Kakuganji, Tsuruoka, Yamagata, Japan. ³²Barrios, JETS/Jacobs, Houston, TX, USA. ³³Southeastern Universities Research Association, Washington, DC, USA. ³⁴Department of Earth and Environmental Sciences, University of Rochester, Rochester, NY, USA. ³⁵Department of Geology, School of Earth and Environment, Rowan University, Glassboro, NJ, USA. ³⁶Department of Earth and Planetary Sciences, American Museum of Natural History, New York, NY, USA. ³⁷These authors contributed equally: Daniel P. Glavin, Jason P. Dworkin.

✉ e-mail: daniel.p.glavin@nasa.gov



Extended Data Fig. 1 | APPI(+) ionization FTICR-MS analysis of Benu (OREX-803006-0) compared to Murchison and Ryugu (A0106). **a**, The low oxygenated molecules observed in the Benu methanol extract as illustrated in the Van Krevelen diagram. **b**, Details around nominal mass $m/z = 319$ with the annotation of some m/z signals. The H/C versus m/z diagrams of **c**, Benu and **d**, Ryugu,

showing the lower molecular mass and higher relative abundance of CHN in the Benu sample also in oxygen poor molecules. Colored annuli enclose the total number of molecules assigned by mass, with colors indicating the relative ratios of the chemical families.



Extended Data Fig. 2 | LC-HRMS chromatograms showing the elution of C_2 to C_{11} amino acids in the acid-hydrolyzed, hot-water extracts of the procedural blank, Bennu (OREX-803001-0), and Murchison. The 45–110 min regions of the LC-HRMS single-ion mass chromatograms corresponding to the *o*-phthalaldehyde/*N*-acetyl-L-cysteine (OPA/NAC) derivatives of C_2 to C_{11} aliphatic primary amino acids in positive ion mode via heated electrospray ionization and a 5 ppm mass accuracy with corresponding m/z values as follows: **C_2** : $m/z = 337.08527$; **C_3** : $m/z = 351.10092$; **C_4** : $m/z = 365.11657$; **C_5** : $m/z = 379.13222$; **C_6** : $m/z = 393.14787$; **C_7** : $m/z = 407.16352$; **C_8** : $m/z = 421.17917$; **C_9** : $m/z = 435.19482$; **C_{10}** : $m/z = 449.21047$; and **C_{11}** : $m/z = 463.22612$. Similar single-ion chromatograms were obtained for the non-hydrolyzed water extracts. Peaks were identified by comparisons of their retention times and exact monoisotopic masses with

those in the amino acid standard analyzed on the same day, and are designated by peak number as follows: (9) glycine, (10) β -alanine, (11) γ -amino-*n*-butyric acid, (12) D- β -aminoisobutyric acid, (13) L- β -aminoisobutyric acid, (14) D-alanine, (15) L-alanine, (16) D- β -amino-*n*-butyric acid, (17) L- β -amino-*n*-butyric acid, (18) δ -aminovaleric acid, (19) α -aminoisobutyric acid, (20) D,L- α -amino-*n*-butyric acid, (21) D-isovaline, (22) (S)-3-aminopentanoic acid, (23) ϵ -amino-*n*-caproic acid, (24) L-isovaline, (25) (R)-3-aminopentanoic acid, (26) L-valine, (27) D-valine, (28) D-norvaline, (29) L-norvaline, (30) L-isoleucine, (31) 8-amino-octanoic acid, (32) D-isoleucine, (33) D-leucine, and (34) L-leucine. Note: the C_7 – C_{11} traces for the procedural blank and Bennu analyses feature spurious signal spikes that are due to instrumental background noise and do not represent analyte peaks.

Extended Data Table 1 | Total C, N, and H contents and stable isotopic compositions of Bennu aggregate samples, compared with selected CCs and Ryugu samples (A0106 and C0107)

Samples	C (wt.%)	$\delta^{13}\text{C}$ (‰)	N (wt.%)	$\delta^{15}\text{N}$ (‰)	H (wt.%)	δD (‰)	N/C (atomic)	H/C (atomic)
Bennu (OREX-500002-0, Avionics Deck)								
OREX-501034/35/38-0 (fines, <0.1 mm) ^a	4.7 ± 0.4	2.7 ± 0.1	0.24 ± 0.02	74.6 ± 0.1	0.85 ± 0.04	330 ± 4	0.044 ± 0.005	2.2 ± 0.2
OREX-501036/37/39-0^b (fines, <0.1 mm) ^c	4.7 ± 0.4	3.2 ± 0.1	0.23 ± 0.02	75.5 ± 0.1	0.90 ± 0.04	315 ± 2	0.042 ± 0.005	2.3 ± 0.2
OREX-501040/41-0^b (intermediate, 0.2 mm) ^c	4.7 ± 0.4	−0.5 ± 0.1	0.24 ± 0.02	57.1 ± 0.1	0.93 ± 0.05	305 ± 2	0.044 ± 0.005	2.4 ± 0.2
Bennu (OREX-800031-0, TAGSAM)								
OREX-803007-0^b (aggregate, <0.5 mm) ^a	4.5 ± 0.2	3.3 ± 0.9	0.25 ± 0.01	82 ± 15	0.93 ± 0.05	344 ± 13	0.048 ± 0.003	2.5 ± 0.2
OREX-803001-103 (residue after water extraction @ 100°C 24h) ^a	4.2 ± 0.2	−2.2 ± 0.6	0.20 ± 0.01	58.0 ± 0.8	1.02 ± 0.03	294 ± 3	0.041 ± 0.003	2.9 ± 0.2
OREX-803001-112 (hot-water extract) ^d	-	−9 ± 3	-	180 ± 47	n.d.	n.d.	-	n.d.
Murchison (CM2)								
Murchison (UIC) (powder, <0.2 mm) ^a	1.97 ± 0.08	−3.5 ± 0.2	0.12 ± 0.01	43.6 ± 0.2	0.97 ± 0.06	−19 ± 7	0.052 ± 0.005	5.9 ± 0.4
Murchison (UIC) (residue after water extraction @ 100°C 24h) ^a	1.78 ± 0.07	−10.4 ± 0.2	0.09 ± 0.01	33.1 ± 0.2	1.02 ± 0.06	−51 ± 3	0.043 ± 0.005	6.8 ± 0.5
Murchison (UIC) (hot-water extract) ^d	-	23 ± 9	-	55 ± 8	n.d.	n.d.	-	n.d.
Tarda and Tagish Lake (C2_{ung})								
Tarda (EPL)^e (powder, <0.2 mm) ^a	3.78 ± 0.09	8.4 ± 0.2	0.23 ± 0.01	55.7 ± 0.2	1.02 ± 0.05	492 ± 4	0.052 ± 0.003	3.2 ± 0.2
Tarda (RV)^f (powder, <0.2 mm) ^a	3.65 ± 0.16	5.1 ± 0.3	0.19 ± 0.01	50.6 ± 0.1	0.67 ± 0.08	520 ± 4	0.045 ± 0.003	2.2 ± 0.3
Tagish Lake (5b)^g (powder, <0.2 mm)	4.11 ± 0.12	10.1 ± 0.3	0.24 ± 0.01	76.2 ± 0.3	0.945 ± 0.003	508 ± 4	0.050 ± 0.003	2.7 ± 0.1
Tagish Lake (11h)^g (powder, <0.2 mm)	4.13 ± 0.12	9.4 ± 0.3	0.19 ± 0.01	62.6 ± 0.3	0.872 ± 0.004	557 ± 6	0.039 ± 0.002	2.5 ± 0.1
Ryugu (Hayabusa2)								
Ryugu (A0106)^h (aggregate, <1 mm)	3.76 ± 0.14	−0.6 ± 2.0	0.16 ± 0.01	43.0 ± 9.0	1.14 ± 0.09	252 ± 13	0.036 ± 0.003	3.6 ± 0.3
Ryugu (C0107)ⁱ (aggregate, <1 mm)	3.59 ± 0.47	1.2 ± 10.0	0.14 ± 0.01	36.8 ± 3.6	1.05 ± 0.10	269 ± 13	0.033 ± 0.005	3.5 ± 0.6

^aSample heated at 120°C for 48 h under Ar (<0.1 ppm H₂O and O₂) in a glovebox, and then kept there at room temperature for 66 h without exposure to atmosphere prior to EA-IRMS analysis.

^bData from ref. 5.

^cSample under Ar in glovebox at room temperature without any exposure to atmosphere prior to EA-IRMS analysis.

^dWater extract first acidified by adding 2 µL of 6 M HCl to the extract (~71 µL) to preserve volatile ammonia and amines in a tin capsule and then dried under vacuum at room temperature for 2 h prior to Nano EA-IRMS analysis. The total C and N abundances (nmol) in the OREX-803001-112 and Murchison dried water extracts were also measured and are shown in Supplementary Table 4. Based on mass balance calculations accounting for the mass loss of C and N and change in their EA-IRMS isotopic compositions from the aggregate during extraction, the water extract should be even more isotopically enriched in ¹³C and ¹⁵N ($\delta^{13}\text{C} \sim +80\%$ and $\delta^{15}\text{N} \sim +178\%$; Supplementary Data Table 4). The lower $\delta^{13}\text{C}$ is likely due to the loss of carbonates and carboxylic acids from the acidification.

^eTarda (EPL) meteorite sample obtained by the Carnegie Earth and Planets Laboratory (EPL).

^fTarda (RV) meteorite sample provided by meteorite dealer Roberto Vargas (RV).

^gData from ref. 61. Only the errors for H reported. The precision for C and N elemental analyses was estimated to be 3% of the reported values and the precision of the C and N isotope measurements was estimated to be ±0.3‰ based on the highest variability observed in standards and replicate analyses.

^hData from ref. 20.

ⁱData from ref. 33.

n.d. = not determined.

Extended Data Table 2 | Blank-subtracted free abundances of ammonia, amines, and amino acids, as measured by LC-FD/ToF-MS, in the hot-water extract of Bennu (OREX-803001-O), compared with selected CCs and Ryugu (A0106)^a

Free Ammonia, Amines & Protein Amino Acids	Bennu (OREX-803001-O)	Murchison (CM2)	Tarda (C2 _{ung})	Orgueil (C11) ^b	Ryugu (A0106) ^b
Ammonia (nmol g ⁻¹)	13,613 ± 357	1,098 ± 144 ~1,600 ^c	n.d.	~4,400 ^c 33,540 ± 3,080 ^d 37,777 ± 6,111 ^e	180 ± 60 ^d
Amines					
Hydrazine	<0.1	<0.1	<0.1	n.r.	n.r.
Methylamine	914 ± 88	1,308 ± 189	30.3 ± 0.2	331.5 ± 0.5	23.8 ± 0.6
Ethylamine	121 ± 7	289 ± 31	7.1 ± 0.2	27.3 ± 2.4	11.4 ± 0.3
Isopropylamine	6.8 ± 0.3	47 ± 5	0.27 ± 0.02	5.1 ± 0.1	0.59 ± 0.03
<i>n</i> -Propylamine	7.0 ± 0.3	60 ± 8	0.32 ± 0.01	4.8 ± 0.1	0.05 ± 0.01
(<i>R,S</i>)- <i>sec</i> -Butylamine	0.47 ± 0.02	3.5 ± 0.4	n.d.	4.9 ± 0.4	<0.1
Isobutylamine	1.3 ± 0.2	18 ± 2	n.d.	<0.7	<0.1
<i>n</i> -Butylamine	1.0 ± 0.3	7.7 ± 1.4	n.d.	1.4 ± 0.1	<0.1
<i>tert</i> -Butylamine	3.4 ± 0.4	11 ± 1	n.d.	1.3 ± 0.2	<0.1
3-Pentylamine	0.34 ± 0.02	5.5 ± 0.4	n.d.	<0.7	<0.1
(<i>R,S</i>)-3-Methyl-2-butylamine	0.44 ± 0.02	7.8 ± 0.9	n.d.	<0.7	<0.1
(<i>R,S</i>)- <i>sec</i> -Pentylamine	0.56 ± 0.02	9.9 ± 0.8	n.d.	<0.7	<0.1
(<i>R,S</i>)-2-Methylbutylamine	0.54 ± 0.02	2.6 ± 0.1	n.d.	<0.7	<0.1
<i>tert</i> -Pentylamine	1.3 ± 0.1	13 ± 1	n.d.	1.1 ± 0.2	<0.1
Isopentylamine	0.53 ± 0.04	0.88 ± 0.01	n.d.	<0.7	<0.1
<i>n</i> -Pentylamine	0.49 ± 0.02	1.2 ± 0.1	n.d.	<0.7	<0.1
<i>n</i> -Hexylamine	0.54 ± 0.02	0.70 ± 0.04	n.d.	<0.7	<0.1
Sum Amines (nmol g⁻¹)	1,060 ± 89	1,786 ± 192	38.0 ± 0.3	377 ± 3	35.8 ± 0.7
Protein Amino Acids					
D,L-Histidine	<0.1	<0.1	<0.1	n.r.	n.r.
D,L-Asparagine	tr.	tr.	<0.1	n.r.	n.r.
D,L-Glutamine	<0.1	<0.1	<0.1	n.r.	n.r.
D,L-Serine	tr.	0.14 ± 0.05	1.70 ± 0.06	0.10 ± 0.03	0.52 ± 0.03
D,L-Arginine	<0.1	<0.1	<0.1	n.r.	n.r.
Glycine	10.1 ± 0.5	11.1 ± 1.2	7.2 ± 0.8	4.0 ± 1.3	1.62 ± 0.04
D,L-Aspartic acid	tr.	tr.	0.9 ± 0.2	0.89 ± 0.48	0.25 ± 0.02
D,L-Glutamic acid	0.01 ± 0.01	0.23 ± 0.02	0.29 ± 0.02	0.12 ± 0.07	0.033 ± 0.001
D,L-Threonine	tr.	0.28 ± 0.02	0.32 ± 0.01	n.r.	<0.1
D,L-Alanine	1.60 ± 0.03	4.1 ± 0.4	0.15 ± 0.04	1.13 ± 0.25	0.17 ± 0.01
D,L-Proline	0.11 ± 0.01	0.89 ± 0.07	0.25 ± 0.03	n.r.	n.r.
D,L-Cysteine	<0.1	<0.1	<0.1	n.r.	n.r.
D,L-Tyrosine	tr.	tr.	0.14 ± 0.12	n.r.	n.r.
D,L-Lysine	<0.1	<0.1	<0.1	n.r.	n.r.
D,L-Methionine	<0.1	<0.1	<0.1	n.r.	n.r.
D,L-Valine	0.081 ± 0.004	0.81 ± 0.06	0.26 ± 0.01	0.04 ± 0.01	<0.2
D,L-Leucine	0.036 ± 0.003	0.13 ± 0.02	0.17 ± 0.01	n.r.	<0.2
D,L-Isoleucine	tr.	0.10 ± 0.01	0.14 ± 0.01	n.r.	<0.1
D,L-Phenylalanine	tr.	tr.	<0.1	n.r.	n.r.
D,L-Tryptophan	<0.1	<0.1	<0.1	n.r.	n.r.
Sum Protein Amino Acids (nmol g⁻¹)	11.9 ± 0.5	17.8 ± 1.3	11.5 ± 0.8	6.3 ± 1.4	2.59 ± 0.05

^aHot-water extracts (100°C for 24 h) of the Bennu aggregate subsample (OREX-803001-O; 25.6 mg), the CM2 Murchison meteorite (University of Chicago at Illinois; 26.3 mg), the C2 ungrouped Tarda meteorite (Roberto Vargas, RV; 723 mg), and Ryugu (A0106; 13.08 mg extracted in water at 105°C for 20 h) were analyzed directly after AccQ-Tag derivatization using liquid chromatography with UV fluorescence and mass spectrometry. Compounds were identified by comparison of elution time and mass spectra to that of standards. Values are the average of three measurements ($n = 3$) with a standard error, $\delta x = \sigma_x \cdot (n)^{-1/2}$. The error in the total sum was determined by adding the absolute errors of the individual compounds in quadrature.

^bAbundances of free amines and protein amino acids in Ryugu (A0106)²⁷. Previously published data of the amine abundances (free and acid-labile) for the C11 Orgueil meteorite⁵⁸ and the free protein amino acid data⁶² are shown.

^cFree ammonia concentrations in water and dichloromethane/methanol (9:1, v/v) extracts of the C11 Orgueil and CM2 Murchison meteorites using gas chromatography mass spectrometry¹⁶.

^dFree ammonia concentrations with 1-sigma error calculated from the NH_4^+ abundances measured in the hot-water extracts (105°C for 20 h) of Ryugu (A0106) and the C11 Orgueil using ion chromatography and mass spectrometry²¹.

^eFree ammonia concentration with 1-sigma error calculated from the NH_4^+ abundance measured using ion chromatography of a cold-water leachate of the C11 Orgueil meteorite after ten sequential extractions in ultrapure water by ultrasonication for 10 min at -2°C to +8°C, followed by centrifugation and filtration²². Abbreviations: n.r. = not reported; n.d. = not determined; tr. = amino acid was tentatively identified at trace levels but was below the limit of quantitation.

Extended Data Table 3 | Free and total amino acid abundances, as measured by LC-FD/ToF-MS and LC-FD/HRMS, in the hot-water extract of Bennu (OREX-803001-0), compared with selected CCs and Ryugu (A0106)

Amino Acid	Bennu (OREX-803001-0)		Murchison (CM2)		Tarda (C2 _{ung})	Orgueil (C11) ^b	Ryugu (A0106) ^c
	Free (nmol g ⁻¹)	Total (nmol g ⁻¹)	Free (nmol g ⁻¹)	Total (nmol g ⁻¹)	Total (nmol g ⁻¹)	Total (nmol g ⁻¹)	Total (nmol g ⁻¹)
Glycine	33 ± 1 (6)	44 ± 1 (6)	28 ± 1 (6)	80 ± 2 (6)	11.2 ± 0.5	11.5 ± 6.0	0.46 ± 0.05
D-Alanine	2.8 ± 0.4 (6)	4.0 ± 0.6 (6)	4.5 ± 0.6 (6)	8.5 ± 1.2 (6)	0.93 ± 0.04	0.90 ± 0.19	0.025 ± 0.006
L-Alanine	2.6 ± 0.4 (6)	3.9 ± 0.6 (6)	4.2 ± 0.6 (6)	11.5 ± 1.5 (6)	1.62 ± 0.06	1.1 ± 0.3	<0.44
β-Alanine	1.6 ± 0.3 (6)	3.3 ± 0.5 (6)	14.2 ± 1.6 (6)	29.2 ± 3.8 (6)	3.8 ± 0.2	30.7 ± 7.6	3.3 ± 0.1
D-Serine	0.21 ± 0.09 (6)	0.18 ± 0.03 (6)	0.38 ± 0.07 (6)	0.54 ± 0.08 (6)	0.21 ± 0.01	<0.01	0.06 ± 0.01
L-Serine	0.24 ± 0.01 (6)	≤0.7 ^a (6)	0.4 ± 0.1 (6)	3.6 ± 0.6 (6)	0.78 ± 0.03	<0.01	0.18 ± 0.03
D-Isoserine	<0.01 (3)	0.027 ± 0.004 (3)	0.057 ± 0.003 (3)	0.51 ± 0.02 (3)	n.d.	n.r.	n.r.
L-Isoserine	<0.01 (3)	0.026 ± 0.004 (3)	0.065 ± 0.008 (3)	0.51 ± 0.02 (3)	n.d.	n.r.	n.r.
D-Aspartic Acid	0.94 ± 0.12 (6)	1.35 ± 0.14 (6)	0.69 ± 0.11 (6)	2.4 ± 0.3 (6)	0.42 ± 0.01	0.41 ± 0.23	<0.06
L-Aspartic Acid	0.79 ± 0.16 (6)	1.22 ± 0.12 (6)	0.73 ± 0.15 (6)	5.1 ± 0.6 (6)	0.95 ± 0.03	0.41 ± 0.21	0.02 ± 0.01
D-Threonine	<1 (6)	<0.2 (6)	<0.2 (6)	1.2 ± 0.4 (6)	n.d.	n.r.	<0.02
L-Threonine	<1 (6)	<0.2 (6)	<1 (6)	13 ± 4 (6)	n.d.	n.r.	<0.04
D,L-α-ABA	0.55 ± 0.03 (6)	0.80 ± 0.02 (6)	1.90 ± 0.04 (6)	3.23 ± 0.08 (6)	0.19 ± 0.01	0.69 ± 0.48	<0.02
D-β-ABA	0.34 ± 0.05 (6)	0.55 ± 0.08 (6)	1.9 ± 0.3 (6)	3.4 ± 0.5 (6)	0.58 ± 0.02	2.1 ± 1.1	0.32 ± 0.01
L-β-ABA	0.33 ± 0.05 (6)	0.53 ± 0.08 (6)	1.6 ± 0.2 (6)	2.8 ± 0.4 (6)	0.60 ± 0.02	1.8 ± 0.6	0.32 ± 0.01
γ-ABA	0.37 ± 0.04 (6)	3.03 ± 0.13 (6)	2.9 ± 0.4 (6)	9.2 ± 0.7 (6)	2.9 ± 0.1	2.7 ± 1.3	3.5 ± 0.2
α-AIB	0.21 ± 0.03 (6)	0.61 ± 0.05 (6)	18.6 ± 0.9 (6)	21.0 ± 1.2 (6)	0.54 ± 0.03	3.3 ± 1.4	0.38 ± 0.02
D-β-AIB	0.087 ± 0.002 (3)	0.16 ± 0.01 (3)	0.60 ± 0.01 (3)	1.25 ± 0.06 (3)	n.d.	tr.	0.20 ± 0.01
L-β-AIB	0.088 ± 0.001 (3)	0.16 ± 0.01 (3)	0.66 ± 0.01 (3)	1.30 ± 0.07 (3)	n.d.	tr.	0.17 ± 0.02
D-Glutamic Acid	0.08 ± 0.02 (6)	0.79 ± 0.06 (6)	0.64 ± 0.07 (6)	3.5 ± 0.3 (6)	0.79 ± 0.04	0.32 ± 0.11	<0.03
L-Glutamic Acid	0.07 ± 0.01 (6)	≤0.8 ^d (6)	0.85 ± 0.11 (6)	10.6 ± 1.1 (6)	7.04 ± 0.14	0.56 ± 0.15	<0.03
D-Valine	0.08 ± 0.01 (6)	0.16 ± 0.01 (6)	0.93 ± 0.09 (6)	1.64 ± 0.04 (6)	0.05 ± 0.01	0.19 ± 0.05	<0.07 (0.026) ^f
L-Valine	0.09 ± 0.01 (6)	0.32 ± 0.06 (6)	1.0 ± 0.1 (6)	4.3 ± 0.2 (6)	0.81 ± 0.01	0.48 ± 0.02	<0.06 (0.056) ^f
D-Isovaline	0.015 ± 0.003 (6)	0.080 ± 0.007 (6)	5.3 ± 1.2 (6)	5.97 ± 0.70 (6)	0.04 ± 0.01	0.31 ± 0.03	<0.05 (0.053) ^f
L-Isovaline	0.016 ± 0.002 (6)	0.074 ± 0.006 (6)	5.4 ± 1.0 (6)	5.90 ± 0.80 (6)	0.04 ± 0.01	0.42 ± 0.02	<0.05 (0.047) ^f
D-Norvaline	0.024 ± 0.004 (6)	0.052 ± 0.005 (6)	0.15 ± 0.01 (6)	0.246 ± 0.006 (6)	<0.1	0.11 ± 0.01	<0.04 (0.017) ^f
L-Norvaline	0.029 ± 0.007 (6)	0.051 ± 0.004 (6)	0.14 ± 0.01 (6)	0.245 ± 0.006 (6)	<0.1	0.12 ± 0.01	<0.04 (0.017) ^f
(R)-3-APA	0.038 ± 0.004 (6)	0.074 ± 0.003 (6)	0.32 ± 0.04 (6)	0.68 ± 0.04 (6)	0.06 ± 0.01	1.6 ± 0.1 ^e	<0.06
(S)-3-APA	0.038 ± 0.003 (6)	0.072 ± 0.002 (6)	0.33 ± 0.04 (6)	0.73 ± 0.03 (6)	0.06 ± 0.01		<0.08
D,L- and D,L- <i>allo</i> -3-A-2-MBA	0.09 ± 0.01 (3)	0.25 ± 0.01 (3)	0.29 ± 0.01 (3)	2.08 ± 0.03 (3)	1.10 ± 0.01	0.55 ± 0.03	tr.
3-A-3-MBA	<0.01 (3)	0.1 ± 0.1 (3)	0.25 ± 0.03 (3)	0.25 ± 0.05 (3)	0.23 ± 0.05	<0.26	tr.
3-A-2,2-DMPA	0.04 ± 0.01 (3)	0.125 ± 0.002 (3)	0.82 ± 0.03 (3)	2.50 ± 0.01 (3)	0.05 ± 0.01	0.59 ± 0.03	0.055 ± 0.002
D,L-3-A-2-EPA	0.04 ± 0.01 (3)	0.121 ± 0.001 (3)	0.25 ± 0.01 (3)	0.98 ± 0.01 (3)	<0.1	1.5 ± 0.1	tr.
D,L-4-APA	0.02 ± 0.01 (3)	0.500 ± 0.003 (3)	0.21 ± 0.01 (3)	1.37 ± 0.02 (3)	0.14 ± 0.01	2.4 ± 0.2	tr.
D,L-4-A-2-MBA	0.02 ± 0.01 (3)	0.51 ± 0.01 (3)	0.11 ± 0.01 (3)	1.62 ± 0.06 (3)	0.11 ± 0.01	1.5 ± 0.1	<0.17
D,L-4-A-3-MBA	<0.01 (3)	0.046 ± 0.001 (3)	0.02 ± 0.01 (3)	0.190 ± 0.003 (3)	0.03 ± 0.01	2.8 ± 0.1	tr.
5-APA	0.06 ± 0.01 (6)	1.01 ± 0.04 (6)	1.2 ± 0.3 (6)	6.4 ± 0.3 (6)	1.26 ± 0.02	1.2 ± 0.2	1.2 ± 0.1
D-Leucine	tr. (3)	0.09 ± 0.01 (3)	<0.1 (3)	0.9 ± 0.2 (3)	n.d.	n.r.	<0.05
L-Leucine	<0.3 (3)	<0.3 (3)	<0.1 (3)	1.3 ± 0.5 (3)	n.d.	n.r.	<0.06
D-Isoleucine	tr. (6)	0.069 ± 0.005 (6)	0.25 ± 0.05 (6)	0.4 ± 0.1 (6)	n.d.	n.r.	<0.04
L-Isoleucine	<0.1 (6)	≤0.4 ^d (6)	0.24 ± 0.02 (6)	2.3 ± 0.2 (6)	n.d.	n.r.	<0.04
ε-Amino- <i>n</i> -caproic acid	<0.1 (3)	0.19 ± 0.07 (3)	0.24 ± 0.06 (3)	0.9 ± 0.1 (3)	<0.1	0.82 ± 0.79	4.5 ± 2.6
Sum C₂ to C₆ amino acids	45 ± 1	70 ± 2	101 ± 2	253 ± 7	37 ± 1	71 ± 10	15 ± 3

^aHot-water extracts (100°C for 24 h) of the Bennu aggregate subsample (OREX-803001-0; 25.6 mg), the CM2 Murchison meteorite (University of Illinois Chicago, UIC; 26.3 mg), the C2 ungrouped Tarda meteorite (Roberto Vargas, RV; 723 mg), the C11 Orgueil meteorite (Musée National d'Histoire Naturelle de Paris; 1 g), and Ryugu (A0106; 13.08 mg extracted in water at 105°C for 20 h) were analyzed after desalting using cation exchange chromatography and *o*-phthalaldehyde/*N*-acetyl-L-cysteine (OPA/NAC) derivatization (15 min). The OPA/NAC amino acid derivatives were identified using liquid chromatography with UV fluorescence detection/time-of-flight mass spectrometry (LC-FD/ToF-MS) and LC-FD/high-resolution mass spectrometry (HRMS). The reported uncertainties in the individual amino acid concentrations in OREX-803001-0 and Murchison are based on the averages of three or six individual measurements (n) from both instruments with a standard error, $\delta x = \sigma_x \cdot (n)^{-1/2}$. The error in the total sum was determined by adding the absolute errors of the individual compounds in quadrature.

^bData from ref. 59.

^cData from ref. 27, unless otherwise noted.

^dNon-blank corrected value given as an upper limit for the concentration in the sample extract due to peak areas near background levels and ambiguity associated with the procedural blank contribution to the sample peak. Values included in the sum.

^eCombined abundance of D- and L-enantiomers. Enantiomers were separated but could not be identified due to lack of optically pure standards.

^fSingle measurement made by 3D HPLC with UV fluorescence detection from ref. 20.

Abbreviations: tr. = trace, amino acid tentatively identified above background but was below the limit of quantitation; n.r. = not reported; n.d. = not determined; A = amino; ABA = amino-*n*-butyric acid; AIB = aminoisobutyric acid; APA = aminopentanoic acid; DMPA = dimethylpropanoic acid; EPA = ethylpropanoic acid; MBA = methylbutanoic acid.

Extended Data Table 4 | Summary of the D/L ratios and corresponding L-enantiomeric excesses (L_{ee}) of protein and non-protein amino acids measured in Bennu (OREX-803001-O) and Murchison hot-water extracts

Amino Acid (# of analyses)	Bennu (OREX-803001-O)				Murchison (CM2)			
	Free		Total		Free		Total	
	D/L	L_{ee} (%)	D/L	L_{ee} (%)	D/L	L_{ee} (%)	D/L	L_{ee} (%)
Aspartic Acid (6)	1.2 ± 0.3	-9 ± 13	1.11 ± 0.16	-5.1 ± 7.5	0.95 ± 0.24	2.8 ± 12	0.47 ± 0.08	36 ± 6
Glutamic Acid (6)	1.1 ± 0.3	-7 ± 15	>0.98	<0.6	0.76 ± 0.13	14 ± 7	0.33 ± 0.05	50 ± 4
Serine (6)	0.84 ± 0.17	8 ± 9	>0.26	<59	1.06 ± 0.41	-3 ± 20	0.15 ± 0.03	74 ± 4
Isoleucine (3)	n.d.	n.d.	1.04 ± 0.11	-1.9 ± 5.4	0.87 ± 0.12	6.7 ± 6.6	1.01 ± 0.06	-0.6 ± 3.0
Threonine (6)	n.d.	n.d.	n.d.	n.d.	n.d.	n.d.	0.09 ± 0.04	84 ± 5
Alanine (6)	1.07 ± 0.22	-3 ± 11	1.03 ± 0.16	-1.8 ± 8.0	1.05 ± 0.21	-2.6 ± 10	0.74 ± 0.14	15 ± 8
Valine (6)	0.89 ± 0.17	6 ± 9	0.5 ± 0.1	34 ± 7	0.90 ± 0.12	5.4 ± 6.5	0.38 ± 0.02	45 ± 2
Leucine (3)	n.d.	n.d.	>0.3	<54	n.d.	n.d.	0.72 ± 0.33	16 ± 19
Isoleucine (6)	n.d.	n.d.	>0.17	<71	1.02 ± 0.21	-1 ± 10	0.17 ± 0.05	70 ± 5
β -ABA (6)	1.0 ± 0.2	-2 ± 10	1.03 ± 0.22	-1.6 ± 10.9	1.22 ± 0.25	-10 ± 11	1.21 ± 0.25	-9 ± 12
β -AIB (3)	1.00 ± 0.03	0.05 ± 1.28	0.99 ± 0.07	0.6 ± 3.6	0.92 ± 0.02	4.3 ± 0.8	0.96 ± 0.07	1.9 ± 3.5
Isovaline (6)	0.94 ± 0.23	3 ± 12	1.08 ± 0.13	-3.9 ± 6.2	0.99 ± 0.30	0.6 ± 15	1.02 ± 0.16	-0.8 ± 6.5
Norvaline (6)	0.83 ± 0.24	9 ± 13	1.01 ± 0.09	-0.5 ± 4.9	1.06 ± 0.09	-2.9 ± 4.3	1.00 ± 0.04	-0.2 ± 1.8
3-APA (6)	0.99 ± 0.13	0.4 ± 6.5	1.03 ± 0.05	-1.6 ± 2.6	0.98 ± 0.17	1 ± 9	0.93 ± 0.07	3.6 ± 3.4

^aThe uncertainties for the D/L ratios and L-enantiomeric excesses (L_{ee}) are based on the individual amino acid abundance values and their standard errors propagated through the relevant equations with L_{ee} (%) = $[(L - D)/(L + D)] \times 100$. The large errors in some of the values are due to the relatively small mass of sample available for this study (~10 mg equivalent for the non-hydrolyzed and 6M HCl-hydrolyzed, hot-water extracts) and the relatively low amino acid concentrations in the Bennu aggregate resulting in a low signal-to-noise ratio for the measurements.

Abbreviations: n.d. = not determined due to trace amino acid abundances present at or below the detection limit or due to an interfering compound; ABA = amino-*n*-butyric acid; AIB = aminoisobutyric acid; APA = aminopentanoic acid.

Extended Data Table 5 | Blank-subtracted free abundances of carboxylic acids identified by GC-QqQ-MS analyses of the hot-water extract of Bennu (OREX-803001-0), compared with selected CCs and Ryugu (A0106)^a

Free Carboxylic Acids	Bennu (OREX-803001-0) nmol g ⁻¹	Murchison (CM2) nmol g ⁻¹	Tarda (C2 _{ung}) nmol g ⁻¹	Orgueil (CI1) ^b nmol g ⁻¹	Ryugu (A0106) ^c nmol g ⁻¹
Monocarboxylic acids					
Formic acid	4,106 ± 91	3,814 ± 86	416 ± 79	1,404 ± 67	9,466 ± 103
Acetic acid	1,436 ± 72	4,507 ± 43	865 ± 67	2,018 ± 89	5,708 ± 1,536
Propanoic acid	156 ± 8	251 ± 4	94 ± 7	153 ± 6	<0.1
Isobutyric acid	42 ± 2	49 ± 1	23 ± 1	25 ± 1	<0.1
2,2-Dimethylpropanoic acid	40 ± 3	36 ± 1	<0.1	38 ± 2	<0.1
Butyric acid	85 ± 9	120 ± 4	33 ± 3	43 ± 2	<0.1
2-Methylbutyric acid	<0.1	43 ± 2	19 ± 1	17 ± 1	<0.1
Isopentanoic acid	95 ± 7	115 ± 4	22 ± 1	19 ± 1	<0.1
2,2-Dimethylbutyric acid	<0.1	<0.1	<0.1	<0.1	<0.1
3,3-Dimethylbutyric acid	<0.1	<0.1	<0.1	<0.1	<0.1
Pentanoic acid	35 ± 1	44 ± 1	28 ± 1	26 ± 1	<0.1
2-Ethylbutyric/2-Methylpentanoic acid	<0.1	<0.1	<0.1	<0.1	<0.1
3-Methylpentanoic acid	<0.1	<0.1	<0.1	17 ± 1	<0.1
4-Methylpentanoic acid	<0.1	<0.1	<0.1	13 ± 1	<0.1
Hexanoic acid	<0.1	<0.1	33 ± 7	38 ± 1	<0.1
Benzoic acid	346 ± 10	257 ± 3	<0.1	37 ± 1	<0.1
Dicarboxylic acids					
Oxalic acid	844 ± 44	3,603 ± 14	533 ± 53	1,079 ± 38	<0.1 (14) ^d
Malonic acid	<0.1	<0.1	780 ± 169	253 ± 9	<0.1 (0.6) ^d
Succinic acid	<0.1	196 ± 7	52 ± 2	34 ± 1	<0.1 (9.3) ^d
Fumaric/Maleic acid	<0.1	<0.1	<0.1	28 ± 1	<0.1 (1.7) ^d
Glutaric acid	25 ± 1	37 ± 2	31 ± 1	23 ± 1	<0.1 (3.5) ^d
Sum Carboxylic Acids (nmol g⁻¹)	7,210 ± 125	13,072 ± 98	2,929 ± 205	5,263 ± 118	15,203 ± 1,539^e

^aHot-water extracts (100°C for 24 h) of the Bennu aggregate subsample (OREX-803001-0; 25.6 mg), the CM2 Murchison meteorite (University of Chicago at Illinois; 26.3 mg), the C2 ungrouped Tarda meteorite (Roberto Vargas, RV; 723 mg), and Ryugu (A0106; 13.08 mg extracted in water at 105°C for 20 h) were desalted by cation exchange chromatography and then analyzed after 2-pentanol derivatization using gas chromatography with triple quadrupole mass spectrometry. Compounds identified by comparison of elution time and mass spectra to that of standards. Values are the average of three measurements ($n = 3$) with a standard error, $\delta x = \sigma_x \cdot (n)^{-1/2}$. The error in the total sum was determined by adding the absolute errors of the individual compounds in quadrature.

^bData first reported in this study for CI1 Orgueil using the same extraction and derivatization methods as OREX-800031-0 and Murchison.

^cValues measured in a hot-water extract (105°C for 20 h) by gas chromatography mass spectrometry²⁰, unless otherwise noted.

^dValues for dicarboxylic acids in a hot-water extract (105°C for 20 h) measured by capillary electrophoresis high-resolution mass spectrometry²⁷. No errors were reported²⁷.

^eNote that several other mono-, di-, and tricarboxylic acids were identified in the Ryugu (A0106) hot-water extract²⁷ and are not included in this Table, therefore this value is a lower limit for the total abundance of carboxylic acids.

Extended Data Table 6 | Blank-subtracted abundances of N-heterocycles identified by HPLC/HRMS analyses of a 6 M HCl extract of Bennu (OREX-800044-101), compared with selected CCs and Ryugu (A0106)^a

N-Heterocycles	Bennu (OREX-800044-101) nmol g ⁻¹	Murchison (CM2) ^b nmol g ⁻¹	Orgueil (CI1) ^c nmol g ⁻¹	Ryugu (A0106) ^d nmol g ⁻¹
Canonical Nucleobases				
Uracil	0.90 ± 0.06	1.90 ± 0.04	0.24	0.10 ± 0.05
Thymine	0.57 ± 0.04	0.59 ± 0.04	n.r.	n.r.
Cytosine	0.31 ± 0.07	0.26 ± 0.01	n.r.	n.r.
Adenine	0.26 ± 0.12 ^e	0.90 ± 0.03	0.05	n.r.
Guanine	0.12 ± 0.07	4.3 ± 0.7	0.13	n.r.
Other Purines and Pyrimidines				
Purine	0.004 ± 0.002	0.033 ± 0.001	0.04	n.r.
Hypoxanthine	0.12 ± 0.05	1.12 ± 0.02	0.04	n.r.
Xanthine	0.40 ± 0.17	1.49 ± 0.09	<0.07	n.r.
Isoguanine	0.13 ± 0.04 ^e	0.62 ± 0.01	n.r.	n.r.
2-Aminopurine	n.d.	0.004 ± 0.001	n.r.	n.r.
8-Aminopurine	n.d.	0.23 ± 0.01	n.r.	n.r.
2,6-Diaminopurine (DAP) + 6,8-DAP ^f	0.17 ± 0.04	0.18 ± 0.01	<0.01	n.r.
1-Methyluracil	0.03 ± 0.01	0.06	n.r.	n.r.
6-Methyluracil	0.39 ± 0.04	0.36	n.r.	n.r.
Other N-Heterocycles				
Imidazole	<i>tentative</i>	16	n.r.	n.r.
2-Imidazole carboxylic acid	0.05 ± 0.01	0.21	n.r.	0.054
4-Imidazole carboxylic acid	0.13 ± 0.01	3.1	n.r.	0.15 ± 0.03
2-Methyl-1H-imidazole carboxylic acid	0.41 ± 0.05	n.r.	n.r.	n.r.
Picolinic acid	<i>tentative</i>	<i>tentative</i>	n.r.	n.r.
Nicotinic acid (vitamin B3)	0.43 ± 0.07	2.5	n.r.	0.40 ± 0.01
Isonicotinic acid	0.17 ± 0.04	1.2	n.r.	0.40 ± 0.16
2-Methylnicotinic acid	0.04 ± 0.01	n.r.	n.r.	n.r.
5-Methylnicotinic acid	0.12 ± 0.03	n.r.	n.r.	n.r.
6-Methylnicotinic acid	0.14 ± 0.03	n.r.	n.r.	n.r.
Sum all Purines (nmol g⁻¹)	1.2 ± 0.2	8.9 ± 0.7	~0.26	-
Sum all Pyrimidines (nmol g⁻¹)	2.2 ± 0.1	3.2 ± 0.1	~0.24	0.10 ± 0.05
Sum all N-Heterocycles (nmol g⁻¹)	4.9 ± 0.3	35 ± 1	~0.48	1.1 ± 0.2
Ratio (Purines/Pyrimidines)	0.55 ± 0.09	2.8 ± 0.2	~1.08	-

^aCompounds identified by comparison of elution time and mass spectra to standards. Values are the average of two measurements ($n = 2$) with a standard error, $\delta x = \sigma_x \cdot (n)^{-1/2}$. The error in the sum was determined by adding the errors of the individual compounds in quadrature.

^bValues represent the combined extractable total abundances in hot-water and 6 M HCl extracts⁶³.

^cValues for purines from a formic acid extract³⁴, and the uracil abundance from water, formic acid, and HCl extracts⁶⁴.

^dValues represent the total abundances in the 6 M HCl hydrolyzed, hot-water extract³³.

^eUpper limit.

^f2,6-DAP and 2,8-DAP co-eluted under the chromatographic conditions used, therefore the sum of abundances is reported assuming both compounds have similar ionization responses and detection efficiencies.

Abbreviations: n.r. = not reported; n.d. = not determined.